

# Vision Toolkit Part 2. Features and Metrics for Assessing Oculomotor Signal: A Review

Quentin Laborde<sup>1,2,\*</sup>, Axel Roques<sup>1,3</sup>, Allan Armougom<sup>2</sup>, Nicolas Vayatis<sup>1</sup>,  
Ioannis Bargiotas<sup>4</sup>, Laurent Oudre<sup>1</sup>

<sup>1</sup> Université Paris Saclay, Université Paris Cité, ENS Paris Saclay, CNRS, SSA,  
INSERM, Centre Borelli, F-91190, Gif-sur-Yvette, France

<sup>2</sup> SNCF, Technologies Department, Innovation & Research, F-93210, Saint Denis,  
France

<sup>3</sup> Thales AVS France, Training & Simulation, F-95520, Osny, France

<sup>4</sup> Université Paris-Saclay, Inria, CIAMS, F-91190, Gif-sur-Yvette, France

Correspondence\*:

Corresponding Author

email@uni.edu

## 2 ABSTRACT

Eye movement analysis provides critical insights across domains such as perception, cognition, neurological diagnostics, and human-computer interaction. However, reliable quantification of oculomotor remains challenging due to the lack of clear boundaries between fixations, saccades, and smooth pursuits, or variability across individuals and contexts. This article reviews methods for segmenting oculometry data into canonical oculomotor events, and the computational tools that can be used to characterize them. Binary segmentation employs mostly threshold-based algorithms and learning-based algorithms to distinguish fixations from saccades. Ternary segmentation additionally considers smooth pursuits using primarily threshold-based approaches and deep learning techniques. The common challenges in the practical application of segmentation algorithms are highlighted, namely parameter sensitivity, noise, and head movement artifacts in mobile eye trackers, and emphasize the need for standardized benchmarks. The usual oculomotor metrics that can be inferred from the canonical movements are described, encompassing temporal, spatial, and kinematic features. The critical insights they provide for cognitive and clinical research in fields such as reading comprehension, neurological disorder diagnostics, and sensorimotor development, are outlined. Finally, relatively underexplored methods from signal processing, including spectral, stochastic, and topological methods, are presented. Their potential in revealing oscillatory patterns and structural complexities in gaze dynamics is detailed. Together, these approaches enhance our understanding of eye movement behavior, with significant implications for psychology, neuroscience, and human-computer interaction.

Keywords: Segmentation algorithm, Oculomotor dynamics, Fixations, Saccades, Smooth-pursuits, Signal processing, Eye-tracking

## 1 INTRODUCTION

Eye movement research has a rich history, beginning with foundational work by Dodge and Cline (1901) in the early 20<sup>th</sup> century. Technological advancements have since enhanced the measurement, storage, and

26 analysis of eye movements, enabling significant progress in understanding their underlying mechanisms.  
27 The growing accessibility of eye-tracking tools has expanded their use across global research laboratories,  
28 fostering specialized subfields like neuroscience, psychology, marketing, and medicine. Each discipline  
29 has provided critical insights, collectively shaping modern eye movement research.

30 A primary goal in eye movement research is to extract metrics that characterize the oculomotor system.  
31 Due to their close link with visual attention, eye movements analysis is a powerful tool for studying  
32 cognitive and behavioral processes. Recent studies have integrated eye movement analysis into cognitive  
33 psychology, exploring areas like language processing, reading, and problem-solving (Rayner, 1998a).  
34 Research has also investigated connections between eye movements, visual attention, and perception  
35 (Collins and Doré-Mazars, 2006; Schütz et al., 2011). Additionally, individual differences in oculomotor  
36 patterns have paved the way for eye movement biometrics (Rigas and Komogortsev, 2016).

37 Clinical research increasingly employs eye movement analysis as a non-invasive method to identify  
38 neural irregularities linked to neurodegenerative and neurological disorders (MacAskill and Anderson,  
39 2016). Distinct oculomotor patterns have been observed in individuals with early-stage Alzheimer's disease  
40 (Fernández et al., 2013) and Parkinson's disease (Wetzel et al., 2011), highlighting their potential as  
41 biomarkers for early diagnosis and disease monitoring. Furthermore, a growing body of evidence explores  
42 oculomotor features in behavioral disorders such as attention deficit hyperactivity disorder (ADHD) (Fried  
43 et al., 2014) and autism spectrum disorder (ASD) (Klin et al., 2002; Shirama et al., 2016), offering valuable  
44 insights into the neurocognitive mechanisms underlying these conditions.

45 The rapid growth of eye movement research has also brought significant challenges. The increasing  
46 volume of publications can obscure critical insights, while fragmentation across sub-disciplines hinders  
47 effective knowledge integration. As the different research communities pursue distinct objectives,  
48 definitions and methodologies often become highly specialized, which limits their generalizability. This  
49 has contributed to a fragmented conceptual framework within the field. Notably, a recent study highlights  
50 that even fundamental terms such as *fixation* and *saccade* are defined inconsistently, resulting in *conceptual  
confusion* (Hessels et al., 2018). These definitions vary considerably depending on whether the perspective  
51 is functional, oculomotor, or computational, with little consensus even within individual subfields.

53 Beyond conceptual and terminological inconsistencies, the field lacks standardized methods for defining  
54 and extracting eye movement features. Most studies emphasize feature subsets tailored to specific research  
55 questions, and the methodological variability in segmenting raw gaze data into canonical movements —  
56 such as fixations, saccades, and smooth pursuits — undermines reproducibility. The growing availability of  
57 portable, cost-effective eye-tracking devices has facilitated the study of naturalistic behavior in both  
58 laboratory and real-world settings (Hayhoe and Ballard, 2005; Land, 2009). However, the absence  
59 of standardized analysis protocols limits comparability between studies and hinders the integration of  
60 knowledge. This work aims to address these challenges by proposing a unified methodological framework  
61 to improve interoperability across research communities and improve comparison across experimental  
62 contexts.

63 This review focuses on methods for segmenting, extracting and analyzing fixations, saccades, and smooth  
64 pursuits, building on prior comprehensive reviews of fixation and saccade features (Sharafi et al., 2015;  
65 Rigas et al., 2018; Brunyé et al., 2019; Skaramagkas et al., 2021; Mahanama et al., 2022a; Sperling, 2022)  
66 and pursuit-based features (Skaramagkas et al., 2021; Mahanama et al., 2022a; Sperling, 2022). Some  
67 reviews target specific domains, such as emotional and cognitive processes (Skaramagkas et al., 2021)  
68 or decision-making (Sperling, 2022). Additionally, several studies, including Komogortsev et al. (2010b);

69 Birawo and Kasprowski (2022); Startsev and Zemblys (2023), evaluate segmentation algorithms, often  
70 comparing their performance on open-source datasets and proposing quality metrics. This work aligns with  
71 these efforts by reviewing segmentation methods and their associated oculomotor features.

72 Specifically, this review surveys methodologies for quantifying oculomotor system activity and explores  
73 their diverse applications. While not exhaustive due to the breadth and specialization of some methods,  
74 it provides a concise overview of key approaches for characterizing canonical eye movements and their  
75 oculometric signals. The following sections are organized as follows. Section 2 introduces segmentation  
76 algorithms for classifying fixations, saccades, and smooth pursuits. Two primary analytical approaches  
77 are then explored: physiological analysis — Section 3 — which extracts meaningful features like shape,  
78 dynamics, and kinematics from segmented sequences, and signal-based analysis — Section 4 — which  
79 applies time-series descriptors to examine eye movement behavior from a global dynamic perspective.  
80 Although a detailed discussion of metrics is beyond the scope of this review, we aim to provide a unified  
81 framework for oculometric signal analysis.

82 This article is part of a series of four reviews dedicated to methods for analyzing oculomotor signals and  
83 gaze trajectories. The overarching goals of the series are to evaluate the application of eye movement and  
84 gaze analysis techniques across diverse scientific disciplines and to work toward a unified methodological  
85 framework by defining standardized representations and concepts for quantifying eye-tracking data. The  
86 first article in the series, already published in *Frontiers in Physiology* (Laborde et al., 2025), provided an  
87 overview of current knowledge on canonical eye movements, with particular emphasis on distinguishing  
88 findings obtained in controlled laboratory settings from those observed in more natural, head-free  
89 conditions.

## 2 SEGMENTATION ALGORITHMS

90 Three archetypal gaze patterns can typically be observed in eye-tracking data: periods of relative stability,  
91 rapid eye shifts, and slower shifts corresponding to the tracking of moving objects. These are commonly  
92 assumed to reflect the three main canonical oculomotor events that direct gaze movements, namely  
93 fixations, saccades and smooth pursuits. Thus, a necessary preliminary step in eye-movement analysis  
94 is often to identify these canonical events from a continuous stream of gaze data using segmentation  
95 algorithms. Segmentation algorithms employ a number of predefined criteria, based on the underlying  
96 characteristics of the oculomotor events, in order to distinguish them. Such a process aligns with the  
97 traditional neurophysiological view, which postulates that distinct neural mechanisms govern specific  
98 movement types, such as the superior colliculus for saccades or the cerebellum for smooth pursuits.

99 However, the organization of the oculomotor system as a discrete set of events has been questioned,  
100 notably in the context of natural viewing conditions (Steinman et al., 1990). Under ecological conditions,  
101 a richer repertoire of ocular behavior can be observed. This results in potential overlap between the  
102 characteristics of the oculomotor events, which makes the segmentation task more challenging. Therefore,  
103 it seems more appropriate to refer to segmentation algorithms as event classification rather than event  
104 detection, since they merely assign a discrete event type to each data period based on some computationally  
105 inferred features — e.g., velocity thresholds for saccades or duration thresholds for fixations. This  
106 distinction is critical, as misclassification can distort interpretations of visual attention in fields such  
107 as psychology, neuroscience, and human-computer interaction.

108 A major challenge in eye movement segmentation is the dependence on user-defined parameters,  
109 such as velocity thresholds for saccades or minimum fixation durations. Although these events are

110 grounded in physiological phenomena, no theoretical consensus exists on parameter values that definitively  
111 distinguish movement types. For instance, the transition from slow movements, such as smooth pursuits or  
112 drifts, to rapid saccades lacks a clear, physiologically validated threshold. Studies investigating optimal  
113 parameterization for specific algorithms (Blignaut, 2009; Shic et al., 2008) indicate that variations in  
114 parameter settings significantly influence classification outcomes (Komogortsev et al., 2010b; Salvucci  
115 and Goldberg, 2000). This sensitivity hampers reproducibility and can distort findings in fields requiring  
116 precise event classification, such as psychology or human-computer interaction. In psychology, for example,  
117 precision in detecting fixations is crucial for analyzing attention strategies, such as in studies on reading  
118 or visual information processing (Rayner, 1998b). For instance, in experimental paradigms measuring  
119 cognitive load, accurate identification of fixations enables reliable quantification of the time spent on  
120 specific stimuli, thereby revealing underlying attentional processes (Duchowski and Duchowski, 2017). In  
121 human-computer interaction (HCI), precise classification of eye movement events is equally important  
122 for evaluating the usability of user interfaces (Jacob and Karn, 2003). Correct detection of saccades and  
123 fixations, for example, allows for the identification of interface areas that attract users' attention or pose  
124 accessibility issues, directly influencing the design of more intuitive interfaces.

125 Conversely, errors in the detection of fixations or saccades can have significant repercussions on the  
126 interpretation of data in studies in cognitive psychology and human-computer interaction (HCI). As shown  
127 by Duchowski and Duchowski (2017) and Nyström and Holmqvist (2010), erroneous classification of eye  
128 movement events can bias the analysis of attentional processes or user behaviors. For example, a fixation  
129 incorrectly identified as a saccade can distort measures of cognitive load in experimental paradigms, leading  
130 to erroneous conclusions about underlying cognitive mechanisms (Rayner, 1998b). Similarly, in HCI,  
131 imprecise detection of eye movement events can result in an incorrect evaluation of an interface's usability,  
132 affecting recommendations for its optimization (Jacob and Karn, 2003). As such, threshold-based methods,  
133 including velocity or dispersion thresholding, provide computational interpretations of oculomotor events,  
134 but their criteria often vary across studies and implementations, leading to inconsistent classifications of  
135 identical gaze data due to insufficient standardization, which compromises the reproducibility of results in  
136 contexts requiring high precision (Holmqvist et al., 2011).

137 Finally, researchers must consider the coordinate system used when analyzing eye-tracking data,  
138 particularly with mobile eye trackers that permit free head movement. Unlike stationary trackers, which use  
139 a head-referenced coordinate system, mobile trackers record gaze in a world-referenced system, where head  
140 movements can complicate event classification. To avoid such conceptual confusion, researchers should  
141 ensure proper head movement compensation and clearly report their coordinate system. For a detailed  
142 discussion of challenges in defining oculomotor events, see the review by Hessels et al. (2018). Note that  
143 considerations regarding the utilization and transformation of these coordinates in relation to a moving  
144 observer's visual field are addressed in the first part of this review series (Laborde et al., 2025)

145 Although some authors have called for the standardization of eye movement classification algorithms  
146 and evaluation tools (Komogortsev et al., 2010a), Startsev and Zemblys (2023), there is currently no  
147 clear consensus on how to benchmark these methods. This lack of agreement poses challenges to the  
148 development and comparison of new segmentation approaches. To address this gap, several concrete  
149 proposals have been suggested in the literature. First, minimal reporting standards could be established,  
150 requiring authors to clearly specify algorithm parameters, eye-tracker sampling rates, stimulus types, and  
151 data preprocessing steps. Second, the use of shared, openly available datasets would enable reproducible  
152 evaluation across diverse conditions, including static, dynamic, and naturalistic stimuli. Third, benchmark  
153 competitions or challenges could be organized, similar to practices in computer vision and machine

154 learning, where algorithms are tested on identical datasets using standardized metrics such as precision,  
155 recall, F1-score, Cohen's Kappa, and RMSD. By adopting these practices, the field could facilitate  
156 more transparent, reproducible, and comparable assessments of eye movement segmentation algorithms,  
157 ultimately accelerating methodological improvements.

158 In this review, we focus on fixations, saccades, and smooth pursuit eye movements, as these are the  
159 most commonly studied and well-characterized oculomotor events in the literature. Other canonical eye  
160 movement events, such as vergence, optokinetic reflexes, and vestibulo-ocular reflex (VOR), are not  
161 included. These events are less frequently analyzed in eye-tracking studies, and their detection often  
162 requires specialized experimental setups or instrumentation beyond conventional gaze-tracking paradigms.  
163 By concentrating on fixations, saccades, and pursuits, we ensure that the discussion is grounded in well-  
164 supported empirical evidence while acknowledging that additional eye movement types remain an important  
165 direction for future work. Despite these challenges, the following sections provide an overview of widely  
166 used segmentation methods (Salvucci and Goldberg, 2000; Komogortsev and Karpov, 2013; Andersson  
167 et al., 2016).

## 168 2.1 Separating Saccades from Fixations

169 Numerous algorithms have been developed to address the challenge of distinguishing saccades from  
170 fixations, a process known as binary segmentation. This is illustrated in Figure 1, which depicts alternating  
171 periods of relative gaze stability — fixations, marked in purple — and rapid gaze reorientations — saccadic  
172 eye movements. The recording shown in Figure 1 is of exceptionally high quality, with minimal noise or  
173 signal loss. In contrast, real-world eye-tracking data often exhibit lower quality due to several factors. For  
174 instance, blinks or partial eyelid closures interrupt the signal, while head movements or poor participant  
175 stabilization can introduce spatial jitter. Changes in lighting conditions or reflections on glasses can  
176 reduce the accuracy of gaze detection, and low sampling rates or occasional data dropouts may cause  
177 missing or irregular samples. Additionally, physiological variability, such as micro-saccades or pupil size  
178 fluctuations, can further complicate event classification. These factors collectively increase the difficulty of  
179 distinguishing fixations from saccades, emphasizing the need for robust segmentation algorithms that can  
180 tolerate noise and handle incomplete or variable-quality data.

181 Binary segmentation algorithms are broadly categorized into *threshold-based* and *learning-based*  
182 approaches. Threshold-based methods rely on predefined computational criteria, such as velocity or spatial  
183 dispersion, to classify fixations and saccades, ensuring transparent, rule-based classification. In contrast,  
184 learning-based methods, encompassing machine learning and deep learning techniques, infer patterns from  
185 annotated training data, which reflect expert or task-specific interpretations of fixations and saccades. These  
186 annotations may reduce the transparency of classification criteria compared to threshold-based methods  
187 due to their reliance on subjective or context-dependent definitions.

### 188 2.1.1 Threshold-based Algorithms

189 The velocity-threshold identification (I-VT) algorithm (Salvucci and Goldberg, 2000) is a widely adopted  
190 method for distinguishing fixations from saccades in eye movement data. It leverages the distinct velocity  
191 profiles of eye movements: low velocities characterize fixations, while high velocities indicate saccades.  
192 The I-VT algorithm calculates the absolute velocity between consecutive gaze samples and classifies each  
193 sample as a fixation or saccade based on a user-defined velocity threshold. To address the subjectivity  
194 of manual threshold selection, Nyström and Holmqvist (2010) proposed an adaptive I-VT variant that  
195 dynamically computes thresholds for peak velocities and saccade onset/offset detection based on statistical

196 properties of the data. This method incorporates constraints derived from the physical characteristics of eye  
197 movements — such as minimum and maximum velocities, accelerations, and event durations — to filter  
198 noise and enhance classification accuracy.

199 In contrast to velocity-based methods, the dispersion-threshold identification (I-DiT) algorithm offers  
200 an alternative approach by leveraging the tendency of fixation points — characterized by relatively low  
201 velocity — to cluster spatially (Salvucci and Goldberg, 2000; Komogortsev et al., 2010a; Andersson  
202 et al., 2016). The I-DiT algorithm distinguishes fixations from saccades based on the spatial dispersion of  
203 consecutive gaze points within a defined temporal window. Dispersion is quantified by summing the ranges  
204 — *i.e.* the differences between the maximum and minimum values — of the gaze coordinates in both the  
205 horizontal and vertical dimensions. If the resulting dispersion value falls below a predefined threshold, the  
206 corresponding gaze points are classified as a fixation. Otherwise, if the dispersion exceeds the threshold,  
207 the sequence is identified as a saccade.

208 Another notable approach is the minimum spanning tree (MST)-based method (Goldberg and Schryver,  
209 1995; Salvucci and Goldberg, 2000; Komogortsev et al., 2010a; Andersson et al., 2016), which also  
210 employs a dispersion-based strategy to evaluate local gaze dispersion within a temporal window of eye  
211 position data. Unlike traditional methods, MST-based algorithms model gaze points as nodes in a graph,  
212 with edges weighted by the Euclidean distance between corresponding positions. A minimum spanning  
213 tree is constructed — typically using Prim's algorithm (Camerini et al., 1988) — to connect all nodes  
214 while minimizing total edge length. The identification by minimum spanning tree (I-MST) algorithm  
215 classifies gaze points by applying edge-distance thresholds: points connected by edges shorter than the  
216 threshold are grouped as fixation components, while those separated by longer edges are classified as  
217 saccadic components. Thresholds may be applied globally across the graph (Komogortsev et al., 2010a) or  
218 adapted locally based on vertex density (Goldberg and Schryver, 1995). The MST-based approach offers  
219 flexibility, adapts to local data structures, and demonstrates robustness in handling missing or noisy data,  
220 making it suitable for complex eye-tracking datasets.

221 The Density-Threshold Identification (I-DeT) algorithm is an adaptation of the DBSCAN clustering  
222 method (Ester et al., 1996). I-DeT extends DBSCAN by incorporating the temporal dimension of gaze  
223 data, ensuring that segmented events reflect the sequential nature of eye movements. As introduced by Li  
224 et al. (2016), a gaze point is classified as a core point if: (i) at least a minimum number of gaze points  
225 lie within a specified spatial radius of the reference point, forming a local neighborhood; and (ii) these  
226 neighboring points form a temporally contiguous sequence in the gaze dataset. Fixations are identified as  
227 clusters comprising core points and their associated neighborhoods, while non-core, non-neighbor points  
228 are classified as saccades or noise. This integration of spatial and temporal constraints makes I-DeT robust  
229 for segmenting gaze data, though its performance depends on careful parameter tuning to avoid over — or  
230 under — segmentation.

231 Building on classical signal processing, Kalman filter-based algorithms (I-KF) model eye movements as  
232 a dynamic system. The two-state Kalman filter, as proposed by Komogortsev and Khan (2007), represents  
233 eye movements using position and velocity states, assuming linear dynamics and Gaussian noise. The  
234 algorithm operates recursively in two phases: (i) the predict phase, which forecasts the next state based on  
235 the system model, and (ii) the update phase, which refines the prediction using observed data to produce a  
236 more accurate state estimate. Saccade detection employs a Chi-square test (Sauter et al., 1991) to assess  
237 discrepancies between predicted and observed gaze velocities, with a threshold determining whether a  
238 sample is classified as a saccade — high velocity — or fixation — low velocity. This approach excels in  
239 handling noisy data by combining predictive modeling with statistical testing, offering a robust framework

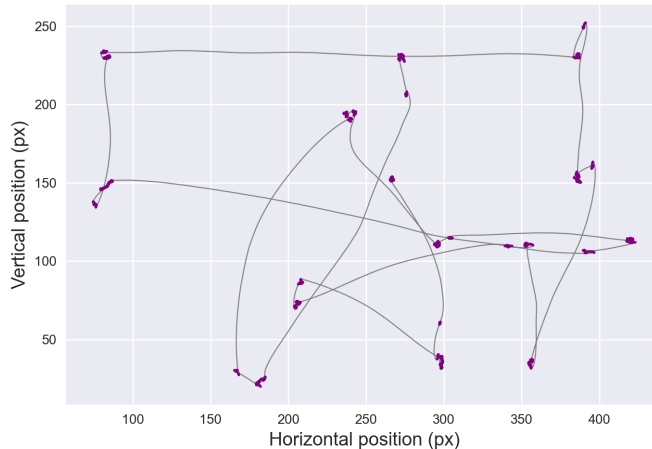


**Figure 1a.** Two-dimensional gaze trajectory

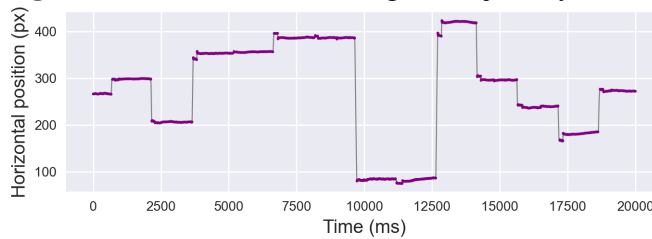


**Figure 1b.** Horizontal gaze positions

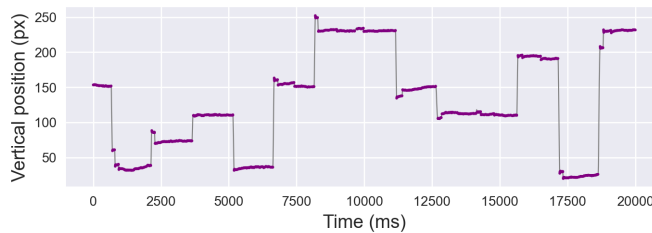


**Figure 1c.** Vertical gaze positions

**Figure 1. Binary Segmentation.** This example shows an oculomotor recording with both fixations and saccades. Fixations, marked in purple, are characterized by low velocity and high density, while rapid ballistic eye movements that redirect gaze between regions of interest are labeled as saccade sequences, marked in gray. These distinctive features are the focus of *binary segmentation algorithms*, which aim to separate fixation from saccade sequences.

240 for eye movement classification applicable in fields such as human-computer interaction and clinical  
241 research.

#### 242 2.1.2 Learning-based Algorithms

243 The Hidden Markov Model Identification (I-HMM) algorithm, introduced by Salvucci and Goldberg  
244 (2000), extends the velocity-threshold identification (I-VT) approach by employing a probabilistic  
245 framework to segment eye movements into fixations and saccades. I-HMM models eye movements  
246 as a sequence of two latent states — fixation and saccade — each characterized by a Gaussian velocity  
247 distribution. Fixations typically exhibit low mean velocity, while saccades are defined by high mean  
248 velocity — e.g. > 200 degrees per second. Transitions between these states are modeled as a first-order

249 Markov process, capturing the temporal dependencies inherent in gaze data. The approach leverages the  
250 Baum-Welch algorithm (Bilmes et al., 1998) to estimate model parameters, including state transition  
251 probabilities and emission distribution parameters — *e.g.* mean and variance of velocity distributions —  
252 from training data. Subsequently, the Viterbi algorithm infers the optimal sequence of states for a given gaze  
253 dataset. Unlike deterministic threshold-based methods like I-VT, I-HMM accounts for noise and sequential  
254 patterns, providing robust segmentation that is particularly effective for noisy or complex eye-tracking  
255 datasets.

256 The Two-Means Clustering Identification (I2MC) algorithm, introduced by Hessels et al. (2017), is  
257 designed to extract fixations from gaze data with high noise levels, such as those recorded from infants. The  
258 algorithm employs two-means clustering — k-means with  $k = 2$  — on a fixed-length temporal window —  
259 typically 200–400 milliseconds — to partition gaze samples into stable — fixation — and rapid — saccade  
260 — clusters based on their spatial coordinates. For each window, the number of transitions between clusters  
261 is calculated, and each gaze sample is assigned a weight inversely proportional to the number of transitions,  
262 reflecting the stability of the cluster assignment. To enhance robustness to noise, this process is applied  
263 across multiple down-sampled versions of the gaze signal. The clustering weights for each gaze sample  
264 are aggregated and averaged to generate a weight signal, which is then thresholded using an empirically  
265 determined cut-off to identify fixation periods, effectively distinguishing fixations from ballistic saccades.  
266 I2MC demonstrates robustness to data loss — *e.g.* due to blinks or tracker errors — and was shown to  
267 outperform seven state-of-the-art algorithms on noisy infant data, making it well-suited for applications in  
268 developmental psychology, clinical research, and longitudinal studies with variable data quality (Hessels  
269 et al., 2017).

270 Building upon established machine learning techniques, Zemblys et al. (2018) introduced the Random  
271 Forest Classifier (I-RF) algorithm to distinguish fixations, saccades, and potentially other eye movement  
272 events from raw gaze data. The I-RF model is trained on a set of 14 features, including spatial measures —  
273 *e.g.* root mean square of sample-to-sample displacement, standard deviation of gaze positions, bivariate  
274 contour ellipse area — and statistical measures — *e.g.* sample dispersion, kurtosis. The random forest  
275 classifier leverages these features to model complex, non-linear relationships, achieving high classification  
276 accuracy. However, a key limitation is the reliance on hand-tagged training data, which is labor-intensive  
277 and hinders scalability. Reproducibility is also challenging, as model performance depends on the quality  
278 and representativeness of training datasets. Additional limitations include the computational cost of feature  
279 extraction and the risk of overfitting to specific datasets. Nevertheless, I-RF is particularly valuable in  
280 eye-tracking research for applications in cognitive psychology, human-computer interaction, and clinical  
281 diagnostics, offering robustness to noise and the potential to detect diverse eye movement types when  
282 trained appropriately.

283 The evaluation of binary segmentation algorithms, which aim to distinguish fixations from saccades, has  
284 been reported in benchmark studies comparing algorithm outputs to human coders using high-frequency  
285 datasets that include static images, text, moving dots, and videos (Andersson et al., 2016). These studies  
286 provide a valuable baseline for assessing segmentation quality. Performances are generally summarized  
287 using metrics such as Cohen's Kappa, which captures agreement with human annotations, or RMSD for  
288 event durations, which reflects temporal precision. However, reported values vary considerably depending  
289 on the dataset, the type of stimulus, and the specific evaluation protocol, making it difficult to directly  
290 compare results across studies.

291 Among threshold-based methods, the velocity-threshold approach (I-VT) typically reaches Kappa values  
292 around 0.65–0.75 for static image datasets but drops markedly in dynamic conditions, particularly for

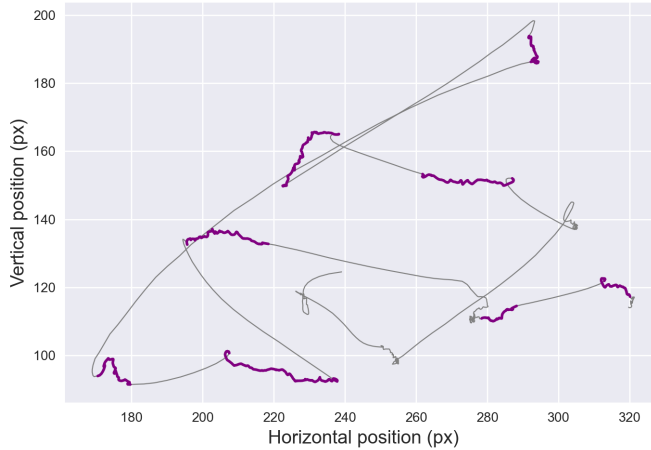


**Figure 2a.** Two-dimensional gaze trajectory

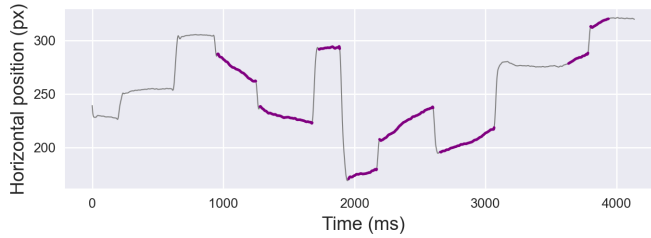


**Figure 2b.** Horizontal gaze positions

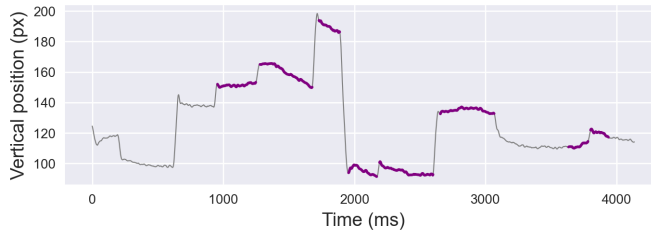


**Figure 2c.** Vertical gaze positions

**Figure 2. Ternary Segmentation.** This example illustrates eye-tracking data, highlighting fixation and saccade phases, as well as smooth pursuit sequences marked in purple. Smooth pursuit sequences are characterized by relatively low velocities coupled with notable directional displacement. These distinguishing features are the focus of *ternary segmentation algorithms*, which aim to isolate pursuit sequences from other phases.

fixations (Andersson et al., 2016). The dispersion-based algorithm (I-DiT) rarely exceeds 0.45 and shows high sensitivity to noise, while I-MST adapts better to missing data but yields modest agreement overall, usually between 0.3 and 0.5 (Andersson et al., 2016). Kalman filter approaches (I-KF) report reasonable performance for saccades — up to 0.6 — but poor fixation detection. More recently, density-based methods such as I-DeT, inspired by clustering techniques, have been proposed as more robust under noise and data loss, though systematic benchmarks remain scarce (Li et al., 2016).

Learning-based approaches tend to report more robust and generalizable performance, particularly in challenging or noisy datasets. Hidden Markov models (I-HMM) achieve balanced results across stimulus types, with Kappa values close to 0.7 for saccades (Andersson et al., 2016). The two-means clustering method (I2MC), developed specifically for noisy infant recordings, reports an average F1-score of 0.83

303 across seven independent datasets, consistently outperforming several threshold-based methods (Hessels  
304 et al., 2017). Random forest classifiers (I-RF) have achieved state-of-the-art sample-level results, with  
305 F1-scores near 0.97 and Kappa values around 0.85 in validation data, though performance decreases to  
306 about 0.70 on independent test sets (Zemblys et al., 2018).

307 In summary, threshold-based methods are attractive for their simplicity and efficiency and remain effective  
308 under controlled static conditions, but they degrade substantially in noisy or dynamic environments.  
309 Learning-based methods demonstrate greater resilience, adaptability, and the ability to model complex  
310 data patterns, although they require annotated training datasets and greater computational resources. It  
311 is important to emphasize that these are reported performances drawn from heterogeneous studies, and  
312 differences in dataset characteristics, sampling frequency, and evaluation protocols likely account for a  
313 substantial part of the observed variability across algorithms.

## 314 2.2 Separating Smooth Pursuits from Fixations and Saccades

315 The detection of smooth pursuit events, characterized by low-velocity, consistent-directionality eye  
316 movements that track moving targets, has received less attention compared to saccade and fixation  
317 classification. This task, known as *ternary segmentation* — classifying fixations, saccades, and smooth  
318 pursuits — is illustrated in Figure 1, which depicts smooth pursuits — marked in purple — alongside  
319 fixations and saccades in high-quality eye-tracking data. Methods for identifying smooth pursuits are  
320 broadly categorized into threshold-based and learning-based approaches. Both approaches encounter the  
321 same limitations outlined in Section 2.1, including sensitivity to predefined thresholds in threshold-based  
322 methods and reliance on annotated training datasets in learning-based methods, which can be labor-intensive  
323 and specific to the dataset. Smooth pursuit detection is particularly challenging in noisy or low-quality data  
324 — e.g. from low-frequency eye trackers or studies involving infants — often necessitating preprocessing  
325 steps such as noise filtering or blink removal to improve accuracy.

### 326 2.2.1 Threshold-based Algorithms

327 Typically, a simple velocity threshold is first applied to isolate saccadic events, followed by a second step  
328 to distinguish between the remaining movements, namely *fixation* and *pursuit* events. A straightforward  
329 but effective method for this task, known as the I-VVT approach, was proposed by Komogortsev and  
330 Karpov (2013). This method builds upon the I-VT algorithm by introducing a second velocity threshold to  
331 specifically isolate fixation events. Any remaining data points are then classified as pursuit events. However,  
332 a potential limitation of this approach is that eye movement velocities can vary between individuals and  
333 even within the same individual depending on the specific task being performed. As such, establishing  
334 universally effective thresholds to differentiate smooth pursuits from fixations — both of which are  
335 low-velocity movements — presents a challenge. This variability can complicate the application of this  
336 algorithm in real-world scenarios, particularly those involving dynamic scenes (Kasneci et al., 2015).

337 To reduce reliance on velocity thresholds, Komogortsev and Karpov (2013) proposed to distinguish  
338 between pursuit and fixation movements using a dispersion threshold combined with a temporal window  
339 — an approach commonly referred to as I-VDT. This method naturally extends the I-DiT approach by  
340 isolating fixation samples based on their spatial proximity. Similarly, Lopez (2009) proposed an alternative  
341 strategy where the standard deviation of movement direction within a time window is used to differentiate  
342 between fixation and pursuit events. This approach provides an additional method for segmentation that  
343 focuses on directional variability rather than relying solely on velocity-based thresholds.

344 The Velocity and Movement Pattern Identification (I-VMP) algorithm, proposed by Lopez (2009),  
345 provides an advanced method for detecting smooth pursuits in eye-tracking data. I-VMP employs a  
346 two-stage approach: it first applies a velocity threshold to isolate saccades, then analyzes the angular  
347 displacement between consecutive gaze points to identify smooth pursuits among low-velocity movements.  
348 Specifically, the angle between the horizontal axis and the line connecting successive gaze points is  
349 projected onto a unit circle, and a Rayleigh score is computed to quantify directional consistency within  
350 a defined temporal window. High Rayleigh scores indicate stable directionality, characteristic of smooth  
351 pursuits, distinguishing them from fixations, which exhibit random or minimal directional changes. While  
352 this method reduces dependence on velocity thresholds compared to traditional approaches, it requires  
353 preprocessing steps, such as noise filtering and blink removal, and knowledge of stimulus motion for  
354 optimal performance.

355 Finally, Santini et al. (2016) introduced a Bayesian decision theory-based approach (I-BDT), specifically  
356 designed for the classification of smooth pursuit eye movements when viewing dynamic stimuli. Unlike  
357 earlier methods that rely on a velocity-based initial step to isolate non-saccadic sequences, this approach  
358 directly separates smooth pursuits from saccades and fixations without the need for an initial velocity  
359 threshold. Grounded in physiological hypotheses, the I-BDT approach incorporates explicit formulas to  
360 compute the likelihoods and priors for each type of eye movement — fixation, saccade, and smooth pursuit.  
361 These formulas enable the efficient classification of eye movement events by applying Bayes' theorem,  
362 offering a probabilistic framework for distinguishing between different types of oculomotor behavior.

### 363 2.2.2 Learning-based Algorithms

364 Fuhl et al. (2018) introduced the Histogram of Oriented Velocities (I-HOV) method, which adapts a  
365 computer vision technique to classify fixations, saccades, and smooth pursuits in eye-tracking data. The I-  
366 HOV algorithm computes velocity-weighted angles between a gaze point and its predecessors or successors  
367 within a defined temporal window, generating a histogram that serves as a meta-representation of local gaze  
368 behavior for each sample. These histograms are used as feature vectors for machine learning algorithms,  
369 such as random forests, k-nearest neighbors, and support vector machines, to classify eye movement  
370 types. Similar to the I-VMP algorithm (Lopez, 2009), I-HOV leverages the consistent directionality and  
371 low-velocity profiles of smooth pursuits to distinguish them from fixations and saccades. While effective  
372 for ternary segmentation, I-HOV relies on high-quality annotated training data and is computationally  
373 intensive. Its performance is also sensitive to noise and the limitations of low-frequency eye trackers, which  
374 may reduce the accuracy of velocity and angle calculations.

375 Recent advances in eye movement classification have leveraged deep learning techniques to distinguish  
376 smooth pursuit sequences from fixations and saccades. One such approach, proposed by Hoppe and  
377 Bulling (2016), employs a convolutional neural network (CNN) combined with data windowing. In this  
378 method, gaze points within each temporal window are transformed into the frequency domain using a  
379 Fourier transform and then input to the CNN, which classifies the eye movement type. Similarly, Fuhl  
380 et al. (2021) introduced a CNN-based method, termed I-CNN, that operates directly on windowed raw eye  
381 data to isolate oculomotor events. These deep learning approaches demonstrate significant effectiveness,  
382 particularly when trained on datasets tailored to specific experimental conditions and eye-tracking devices,  
383 underscoring their potential for robust eye movement classification. However, their performance remains  
384 heavily dependent on the quality and annotation of training data, which can substantially impact model  
385 accuracy and generalizability.

386 Ternary segmentation, tasked with classifying fixations, saccades, and smooth pursuits, presents greater  
387 challenges than binary segmentation due to the subtle low-velocity characteristics of smooth pursuits.  
388 Insights from Komogortsev and Karpov (2013), Santini et al. (2016), Fuhl et al. (2018), and Fuhl et al.  
389 (2021), evaluated on varied datasets with dynamic stimuli, provide a foundation for assessing performance,  
390 although quantitative benchmarks remain less comprehensive than for binary segmentation. Moreover,  
391 the different evaluations were conducted on distinct datasets, making it challenging to provide a reliable  
392 comparative analysis of the various segmentation methods. As such, the following paragraphs will focus  
393 on qualitative considerations.

394 Among threshold-based approaches, extensions of velocity- and dispersion-threshold methods — *e.g.*,  
395 I-VVT, I-VDT — have been applied to pursuits, while variants such as I-VMP incorporate directional  
396 information to reduce velocity ambiguities. Bayesian decision theory (I-BDT) has been reported to  
397 outperform dispersion-based methods (I-VDT) on several dynamic datasets at 30 Hz, leveraging priors  
398 to enhance pursuit detection (Santini et al., 2016). Learning-based methods show greater adaptability.  
399 Histogram-based classification (I-HOV) and convolutional neural networks (I-CNN) have been reported to  
400 provide robust detection of pursuits in noisy or low-resolution dynamic data, outperforming threshold-based  
401 methods in these contexts (Fuhl et al., 2018, 2021).

402 In summary, ternary segmentation highlights the intrinsic difficulty of reliably detecting smooth pursuits,  
403 particularly at low velocities where they overlap with fixations. Threshold-based methods capture faster  
404 pursuits but remain sensitive to noise and sampling rate. Bayesian and direction-based extensions have  
405 been reported to reduce some of these ambiguities, though results vary across datasets. Learning-based  
406 methods appear more promising for handling complex or noisy recordings, especially with CNNs and  
407 histogram-based approaches, yet their effectiveness still depends on the availability of well-annotated  
408 training corpora. Reported performances point to relative strengths of each family of methods, but the  
409 absence of standardized benchmarks makes it difficult to establish a consensus hierarchy of algorithms.

### 3 PHYSIOLOGICAL FEATURES

410 Applying the segmentation algorithms presented in Section 2 produces a sequence of fixations, saccades,  
411 and possibly smooth pursuits from raw gaze data. The following sections will review the most common  
412 metrics found in the literature to describe and analyze these oculomotor events.

413 The fundamental features and metrics for fixations, saccades, and smooth pursuits are summarized in  
414 Tables 1, 2, and 3, respectively. The tables provide a concise description of each feature and references  
415 from the literature that offer guidance for their implementation.

#### 416 3.1 Fixation Measures

417 A fixation is defined as a period during which the gaze is stabilized on a specific spatial location,  
418 projecting visual stimuli onto the *fovea centralis*, the retinal region with maximal photoreceptor density  
419 and visual acuity. Despite attempts to maintain steady fixation on a stationary target, the eyes exhibit  
420 continuous, involuntary micromovements, including microsaccades — rapid, small-amplitude saccades —  
421 drifts — slow, curvilinear deviations — and tremors — high-frequency, low-amplitude oscillations. This  
422 section examines the quantitative features characterizing fixations, including temporal, positional attributes,  
423 and dynamic characteristics. These properties are typically analyzed under head-constrained conditions  
424 using high-resolution eye-tracking systems to isolate oculomotor behavior.

---

425 3.1.1 Temporal Features

426 *Fixation count* is defined as the total number of fixations within a defined time interval or stimulus region.  
427 Despite its simplicity, the fixation count remains a cornerstone metric in eye-tracking research due to its  
428 robustness and interpretability. It is frequently employed in exploratory analyses before applying more  
429 advanced techniques. Fixation count is widely utilized to assess visual attention allocation to regions of  
430 interest (ROIs) in textual or pictorial stimuli (Scheiter and Eitel, 2017), infer the depth and efficiency  
431 of visual processing (Jacob and Karn, 2003; Park et al., 2015), and investigate how expertise influences  
432 oculomotor behavior in visual tasks (Schoonahd et al., 1973; Megaw and Richardson, 1979).

433 Pioneering work by Goldberg and Kotval (1999) highlighted that a higher number of fixations directed at  
434 a stimulus often indicates inefficiency in the search for relevant information. As such, fixation count has  
435 been used in eye-tracking studies to identify visual regions that attract more attention or to infer the amount  
436 of cognitive effort required for a particular task. For example, in challenging tasks such as source code  
437 reading, a higher fixation count could signify increased visual effort and processing time (Binkley et al.,  
438 2013; Sharif et al., 2012). The *fixation count* is often expressed per unit of time or relative to a specific task  
439 or sub-task. For example, in reading tasks, the *fixation count* can be normalized to the length of the text by  
440 dividing the number of fixations by the number of words (Sharafi et al., 2015).

441 Another critical metric, *fixation duration*, quantifies the temporal dynamics of gaze behavior. Typical  
442 fixations last between 200 to 300 milliseconds; however, longer durations on a stimulus may indicate greater  
443 processing complexity (Jacob and Karn, 2003; Krejtz et al., 2016b; Liu and Chuang, 2011). This metric  
444 is frequently employed in eye-tracking studies to examine complex cognitive functions such as reading  
445 comprehension (Raney et al., 2014), learning processes (Liu, 2014), and mental workload assessment (Liu  
446 et al., 2022). Furthermore, individual fixation durations may be analyzed independently. A notable example  
447 is the *first fixation duration* during reading, which is a commonly reported linguistic measure used to assess  
448 initial processing of a word or phrase (Inhoff et al., 2000; Underwood et al., 2000).

449 The temporal characteristics of eye fixations are often analyzed in relation to specific regions within the  
450 visual field that are visually explored. These *areas of interest* (AoI), may represent regions particularly  
451 relevant to the task at hand, or with semantical meaning. Under this formalism, fixation duration metrics  
452 are also used, albeit with slight variations. For instance, the *dwell time* is defined as the cumulative duration  
453 of all fixations during a single visit to an AoI. The *total dwell time* sums all *dwell time* within a specific  
454 AoI over the entire experimental session. Additional AoI-specific metrics offer further granularity, such  
455 as the *fixation ratio*, defined as the sum of fixation durations within an AoI divided by the total fixation  
456 duration across all AoIs, or the *average fixation duration* within an AoI, derived by normalizing the sum of  
457 fixation durations by the number of fixations in that AoI. The concept of AoI as a symbolic tool will be  
458 explored in greater detail in the *Areas of Interest* part of this review series (Part 4).

---

459 3.1.2 Position and Drift

460 The location of visual fixations is widely studied across various contexts, as it is often assumed to  
461 reflect the allocation of visual attention (Findlay and Gilchrist, 2003). A robust method for modeling the  
462 central position of fixations is the fixation centroid, calculated by averaging the coordinates of gaze points  
463 within individual fixation sequences. Analyzing the spatial distribution of these centroids provides valuable  
464 insights into the regions of a stimulus that are prioritized during task-specific processing, offering direct  
465 evidence of underlying cognitive processes (Henderson, 2003; Rayner, 1998a).

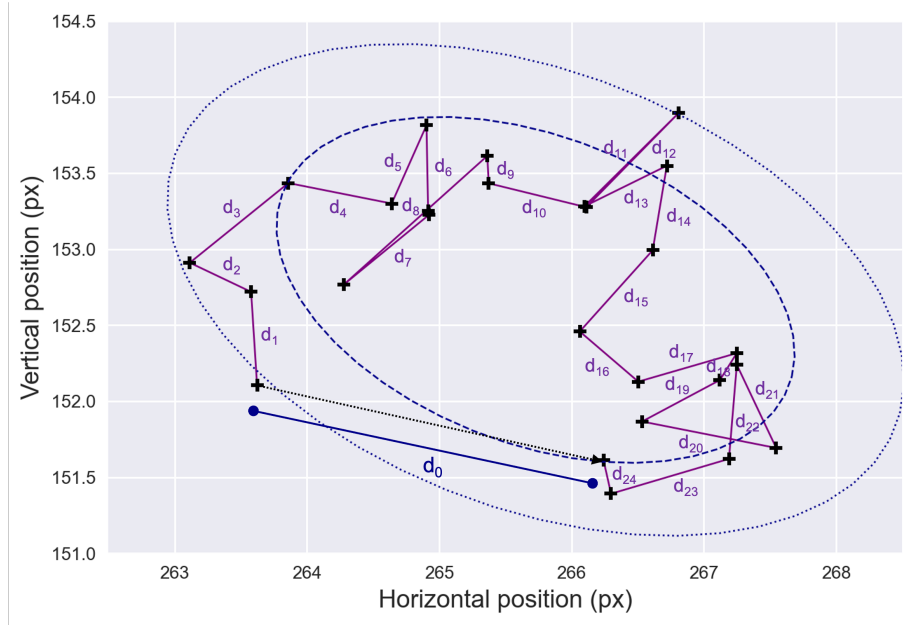


**Figure 3. Fixation Drift and Stability.** An example of gaze data — black crosses — representing a fixation sequence is shown. Note that the raw data have been largely downsampled for presentation clarity. In this illustration, the drift displacement between the starting and ending points of the fixation sequence is denoted as  $d_0$ . The cumulative drift distance is computed by summing the distances  $d_1$  to  $d_{24}$ . Additionally, the figure displays the bivariate contour ellipses for probabilities of 0.68 — blue dashed line — and 0.90 —blue dotted line. The areas enclosed by these ellipses are used to compute the BCEA, a commonly used metric for fixation stability.

466 For instance, in studies related to face processing, analyses of fixation patterns have identified specific gaze  
 467 patterns, such as directing attention to a point just below the eyes (Hsiao and Cottrell, 2008; Peterson and  
 468 Eckstein, 2012). Similarly, in reading tasks, research has shown that both the likelihood of misidentifying  
 469 a word and the time required for identification decrease when the eyes fixate near the center of the word  
 470 (O'Regan and Jacobs, 1992; Brysbaert et al., 1996). These phenomena, known as *optimal viewing position*  
 471 effects, are thought to stem from the rapid decline in visual acuity as retinal eccentricity increases (Nazir  
 472 et al., 1998).

473 While fixational sequences typically exhibit limited eye mobility, the variability in the micro-movements  
 474 can provide valuable information related to oculomotor function. Consequently, several additional features  
 475 — many of which are illustrated in Figure 3 — have been proposed in the literature to better characterize  
 476 fixational micro-movements.

477 As such, the *drift displacement* is calculated as the distance between the starting and ending points of each  
 478 fixation sequence. Similarly, the *cumulative drift distance*, which reflects ocular stability during fixation, is  
 479 obtained by summing the distances between all consecutive fixational data samples from a given fixation  
 480 sequence. Another feature, the *drift mean velocity*, is computed as the average of the first-order position  
 481 derivatives of the fixation data samples and can be used to characterize the minor movements occurring  
 482 during fixation sequences. Together, these measures can provide valuable insights into the stability of eye  
 483 movements during fixation, which may be particularly useful for detecting pathological conditions, such as  
 484 sight impairments and cerebellar diseases (Leech et al., 1977; Schor and Westall, 1984).

Feature name	Description	Reference
Count	Given a set of fixation sequences, computes the number of fixations.	Rigas et al. (2018)
Frequency	Given a set of fixation sequences, computes the number of fixations occurring per second.	Rigas et al. (2018)
Duration	Given a fixation sequence, computes the duration of the sequence.	Rigas et al. (2018)
First duration	Given a set of fixation sequences, computes the duration of the first fixation sequence identified.	Inhoff et al. (2000)
Centroid	Given a fixation sequence, computes centroid position by averaging coordinates of data samples.	Rigas et al. (2018)
Drift displacement	Given a fixation sequence, computes the distance between the starting and ending points of the sequence.	Rigas et al. (2018)
Drift distance	Given a fixation sequence, computes the sum of distances between each data sample within this sequence.	Rigas et al. (2018)
Mean velocity	Given a fixation sequence, computes the mean velocity of data sample within this sequence.	Rigas et al. (2018)
Drift velocity	Given a fixation sequence, computes the drift displacement normalized by the fixation duration.	Rigas et al. (2018)
BCEA	Given a fixation sequence, computes the bivariate contour ellipse area (BCEA) as the area of the elliptical contour that encompasses a given percentage of sample points of the sequence.	Crossland et al. (2004)

**Table 1.** Fixation-based features.

485 Lastly, fixation stability can be quantified by computing the area of the elliptical contour that encompasses  
 486 a given percentage of fixation points (Steinman, 1965; Crossland et al., 2004). Assuming that the fixation  
 487 positions follow a bivariate normal distribution, the dispersion of these positions is represented by an ellipse.  
 488 The *bivariate contour ellipse area* (BCEA) thus provides a measure of fixation stability, with smaller  
 489 values indicating more stable fixation. This metric is considered the current *gold standard* to measure the  
 490 stability of fixation (Crossland et al., 2009) and has been widely used to examine changes in fixational eye  
 491 movements, particularly in clinical contexts (Shaikh et al., 2016; Montesano et al., 2018; Leonard et al.,  
 492 2019; Ghasia and Wang, 2022).

### 493 3.2 Saccade Measures

494 Saccades are rapid, ballistic eye movements that direct the *fovea* toward objects of interest, enabling  
 495 high-acuity vision. Since the inception of eye movement research, the kinematic properties — *e.g.* velocity,  
 496 amplitude — and shape characteristics — *e.g.* trajectory, curvature — of saccadic eye movements have  
 497 been extensively studied using diverse measurement techniques, which we will now review and discuss.

498 In experimental settings, saccadic behavior is investigated using paradigms involving both predictable and  
 499 unpredictable target conditions. The metrics presented in the following sections are designed to quantify  
 500 the dynamics of saccadic eye movements in these two conditions, that is free-viewing scenarios and  
 501 those involving target-based stimuli. These metrics offer critical insights into saccade dynamics and their  
 502 modulation by experimental manipulations.

#### 503 3.2.1 Temporal Features

504 *Saccade duration* is a commonly analyzed metric in eye movement research, with typical values ranging  
 505 from 30 to 70 milliseconds. While these values may vary slightly across studies, various factors have  
 506 been identified in the literature as influencing saccade duration. For example, during coordinated reaching  
 507 movements, saccades that accompany hand motions tend to have shorter durations (Donkelaar et al., 2004;  
 508 Snyder et al., 2002). Conversely, repeated saccades to the same visual stimulus often result in longer

509 durations (Golla et al., 2008; Chen-Harris et al., 2008). The measurement of *saccade duration* typically  
510 involves estimating the onset and offset of the saccade. Given the brief nature of saccadic movements, the  
511 accuracy of this measurement is highly sensitive to the thresholds applied to segment raw gaze data — see  
512 Section 2.

513 In addition to duration, *saccade count* and *saccade rate* — or *saccade frequency* — are widely used  
514 metrics to characterize saccadic sequences. Generally, *saccade frequency* tends to decrease with increasing  
515 task difficulty (Nakayama et al., 2002) or under conditions of fatigue (Van Orden et al., 2000). Like *saccade*  
516 *duration*, *saccade count* is a simple and robust measure commonly employed in studies that investigate  
517 cognitive processes such as reading or scene perception (Inhoff and Radach, 1998). Furthermore, deviations  
518 from typical saccadic temporal characteristics, such as prolonged *saccade duration*, can serve as early  
519 indicators of neural disorders (Ramat et al., 2007).

520 In experimental paradigms that involve target-directed saccades, the temporal aspect of saccadic  
521 movements is frequently examined using *saccadic latency*, which is the time delay between stimulus  
522 onset and saccade initiation. For any given target, while saccade duration, velocity, and amplitude tend to  
523 remain relatively consistent, latency is notably variable across trials, ranging from 100 to 1000 milliseconds  
524 (Liversedge et al., 2011). The distribution of *saccadic latency* is generally skewed toward shorter latencies,  
525 with a long tail representing longer latencies. Additionally, the distribution is often unimodal, although a  
526 second peak — referred to as *express saccades* — can sometimes appear, representing shorter saccadic  
527 responses (Fischer and Weber (1993)).

528 The mean *saccade latency* is typically used to describe the central tendency of reaction times, while the  
529 standard deviation is used to assess variability (Whelan, 2008). However, since the latency distribution  
530 is not Gaussian, these statistics may not fully capture the nature of the distribution. As a result, more  
531 robust statistical measures, such as the median or quantile estimators, are increasingly adopted to describe  
532 saccadic latency distributions more accurately (Vullings, 2018). In clinical contexts, saccadic latency  
533 distributions have shown promise as biomarkers for various neurological conditions. For instance, Michell  
534 et al. (2006) demonstrated that saccadic latency could be used as a diagnostic marker for Parkinson's  
535 disease, highlighting its potential utility in clinical assessments of cognitive and motor dysfunctions.

### 536 3.2.2 Amplitude Features

537 Describing saccade morphology is essential for a comprehensive understanding of eye movement  
538 dynamics. Among the various morphological features, *saccade amplitude* serves as a fundamental and  
539 easily accessible descriptor that reflects the distance the eye travels during a saccadic movement. It is  
540 typically calculated as the spatial distance between the starting and ending points of each identified saccade  
541 sequence. Alternatively, to model the non-linearity of saccade trajectory, the *traveled distance* can be  
542 computed by summing the distances between consecutive saccadic data samples within a saccade sequence.  
543 Lastly, *saccade efficiency*, derived as the ratio of saccadic amplitude to the total distance traveled, is often  
544 used to quantify the complexity and non-linearity of the saccadic trajectory. This metric provides insight  
545 into the degree to which the eye movement follows a straight path versus a more convoluted or inefficient  
546 trajectory.

547 *Saccade amplitude* is highly context-dependent, varying according to the task and visual environment.  
548 For example, in reading tasks, saccades are typically constrained to around 2 degrees of visual angle  
549 horizontally (Rayner et al., 2012). In contrast, during scene perception, the average *saccade amplitude*  
550 increases with the size of the visual stimulus, reflecting the broader spatial search required to process larger  
551 or more complex images (von Wartburg et al., 2007). Cognitive factors also influence *saccade amplitude*,

552 with increases in task difficulty often leading to a decrease in the amplitude of saccadic movements. Phillips  
553 and Edelman (2008) demonstrated that variability in performance during visual scanning tasks was related  
554 to oculomotor variables such as amplitude, with smaller saccades indicating a reduced perceptual span.  
555 Similarly, May et al. (1990) provided evidence that this metric could serve as an indicator of cognitive  
556 workload, with smaller amplitudes reflecting greater cognitive demands. It should also be mentioned that  
557 *saccade amplitude* is closely related to its duration and peak velocity through the *main sequence* relationship  
558 — see Section 3.2.7 for further details. These oculomotor characteristics — amplitude, duration, and peak  
559 velocity — are often analyzed together as they provide complementary insights into the saccadic process.

560 When viewers are instructed to follow a visual target, the *saccadic gain* — the ratio between the amplitude  
561 of the saccade performed and the amplitude of the target displacement — becomes a critical measure.  
562 *Saccadic gain* is particularly useful in assessing saccadic dysmetria, a condition characterized by errors in  
563 saccade accuracy. In neurological studies, saccadic dysmetria is often investigated to identify impairments in  
564 saccadic control. For instance, in overshoot dysmetria, the saccade initially overshoots the target, requiring  
565 a corrective saccade in the opposite direction. While overshoots can occur in healthy individuals, they  
566 typically reduce over time as the oculomotor system adjusts to the target location. Persistent overshooting,  
567 however, is indicative of a cerebellar lesion (Selhorst et al., 1976; Ritchie, 1976). Conversely, undershoot  
568 dysmetria occurs when the initial saccade is too small, and a corrective saccade is required to bring the eye  
569 to the target. Significant undershooting is often associated with basal ganglia disorders, such as Parkinson's  
570 disease (MacAskill et al., 2002) or progressive supranuclear palsy (Troost and Daroff, 1977).

571 More intriguingly, saccadic dysmetria — particularly hypometric saccades — has been proposed as a  
572 potential objective biomarker for neurodegenerative diseases. Abnormally hypometric saccades, along  
573 with other eye movement deficits, have shown promise as early indicators of conditions like Alzheimer's  
574 disease, making them valuable targets for early diagnosis (Fletcher and Sharpe, 1986; Cerquera-Jaramillo  
575 et al., 2018). This highlights the importance of saccade morphology not only for understanding normal  
576 visual behavior but also as a potential tool for identifying and monitoring the progression of neurological  
577 disorders.

### 578 3.2.3 Direction and Curvature

579 The direction of a saccadic trajectory — or sequence of saccades — provides a crucial descriptive measure  
580 of eye movements. This direction is typically quantified as the angle, measured in degrees or radians,  
581 between the horizontal axis and the line connecting the starting and ending points of the saccade. For  
582 instance, Walker et al. (2006) employed *saccadic direction* to examine the effects of target predictability,  
583 while Foulsham et al. (2008) explored the *horizon bias* during natural scene viewing, revealing a prevalent  
584 tendency for horizontal saccades. More recently, studies have employed *saccadic direction* to classify  
585 task-specific gaze patterns, offering valuable insights for designing effective learning strategies (Mozaffari  
586 et al., 2020).

587 However, simple metrics such as amplitude, efficiency — as discussed in Section 3.2.2 — and direction  
588 alone are insufficient for fully capturing the complexity and non-linearity of saccadic trajectories. To  
589 address this gap, several additional features have been developed to better characterize the curvature of  
590 saccadic movements (Ludwig and Gilchrist, 2002).

591 One such metric is *initial deviation*, which measures the angle between the initial direction of the saccade  
592 — computed after a fixed number of time samples, e.g. 20 milliseconds (Van Gisbergen et al. (1987)) — and  
593 the overall direction of the saccade at its endpoint. A limitation of this method is that it assigns varying  
594 curvature values to saccades with identical trajectories but different velocities, because it relies on a fixed

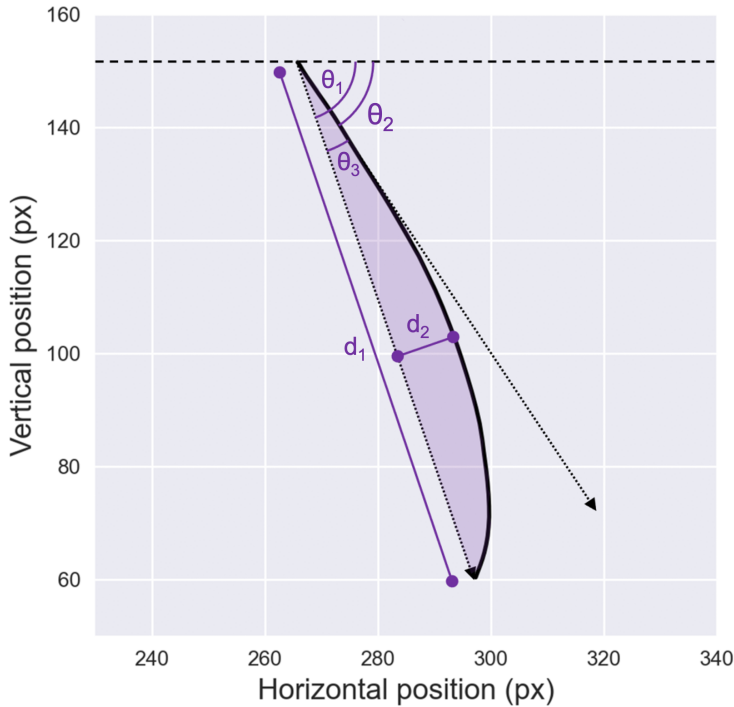


**Figure 4. Saccade Direction and Curvature.** Illustration of various metrics used to describe saccade non-linearity in the literature. The line connecting the starting point and the endpoint of the saccade, with amplitude  $d_1$ , defines the overall saccade direction, denoted as  $\theta_1$ . The initial direction of the saccade, denoted  $\theta_2$ , is calculated after a fixed number of data points. From these two directions, the initial deviation of the saccade, denoted  $\theta_3$ , can be derived. Additionally, the figure highlights the maximum curvature, represented by  $d_2$ , and the area of curvature, indicated by the purple shaded region.

595 time interval. Another common metric is *maximum curvature*, defined as the greatest perpendicular distance  
 596 between a point on the saccadic trajectory and the straight line connecting the starting and ending points  
 597 of the saccade (Smit and Van Gisbergen, 1990). Although widely used, this approach has limitations, as  
 598 it relies on a single point to represent the curvature of a trajectory. This can be especially problematic  
 599 for double-curved saccades, where the trajectory may involve multiple directional changes (Ludwig and  
 600 Gilchrist, 2002).

601 To address these shortcomings, the *area curvature* metric has emerged as a more robust and popular  
 602 approach, as it incorporates the entire trajectory of the saccadic eye movement (Walker et al., 2006). This  
 603 metric is typically calculated by evaluating the area beneath the curve formed by the sampled trajectory,  
 604 relative to the direct distance between the starting and ending points of the saccade. The curvature metrics  
 605 discussed so far are illustrated in Figure 4. Additionally, Ludwig and Gilchrist (2002) proposed deriving  
 606 saccade curvature directly from second- and third-order polynomial fits. Like the *area curvature* approach,  
 607 this method uses the full set of samples from a given saccade, which enhances its robustness by making it  
 608 less sensitive to sampling noise.

609 To investigate the inherent tendency for curvature observed in saccadic movements —particularly  
 610 prominent in oblique saccades (Viviani and Swensson (1982)) — early research primarily focused on  
 611 target location and the type of saccade being performed (Viviani, 1977; Smit and Van Gisbergen, 1990).  
 612 More recent studies, however, have shown that both the direction and magnitude of saccadic curvature can  
 613 be modulated by a variety of factors. Notably, strong correlations have been observed between saccade

614 curvature and the modulation of eye movements by distractors. For example, Doyle and Walker (2001)  
615 found that both reflexive and voluntary saccades tended to curve away from irrelevant distractor stimuli  
616 when a target was presented. Similarly, Sheliga et al. (1997, 1995) demonstrated that saccades deviated from  
617 a previously attended location. These variations in saccadic trajectory have been attributed to antagonistic  
618 interactions between different populations of neurons in the superior colliculus, which help resolve conflicts  
619 caused by competing targets in the vicinity at the onset of movement (McPeek et al., 2003).

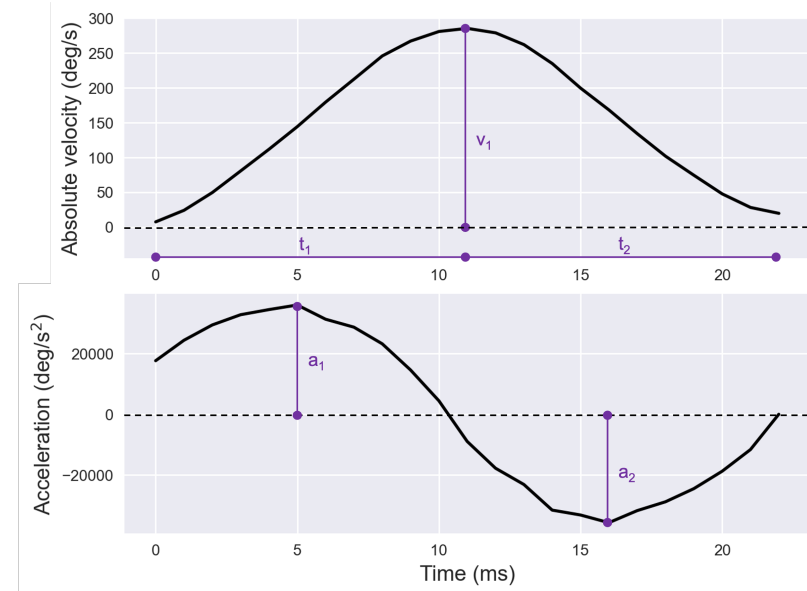
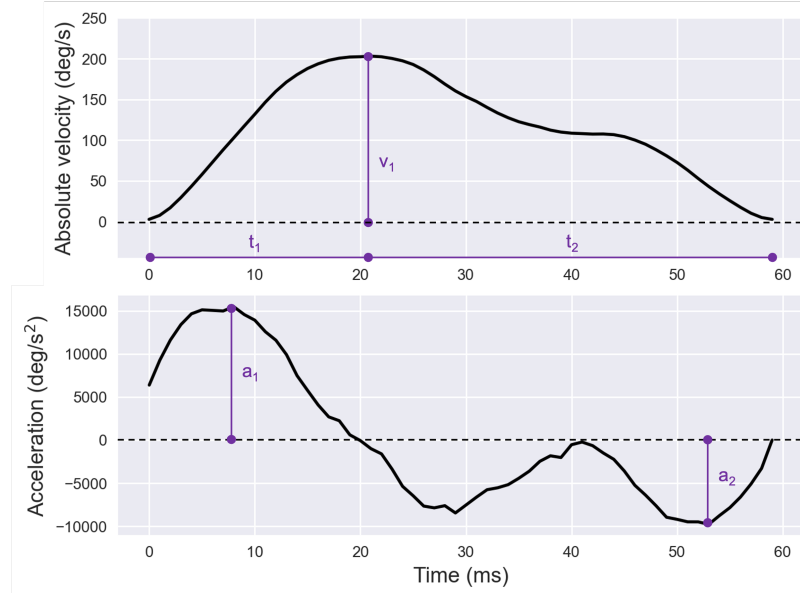
### 620 3.2.4 Velocity Features

621 The velocity waveform of a saccade is generally described as symmetrical with comparable durations for  
622 the acceleration and deceleration phases — Figure 5a. Peak saccadic velocity, the maximum speed attained  
623 during a saccade, typically coincides with the cessation of the neural signal pulse and aligns with the point  
624 of maximum firing rate of burst neurons within the pontine reticular formation that project to oculomotor  
625 neurons (Galley, 1989; Leigh and Zee, 2015). It is noteworthy that average and peak saccadic velocities  
626 are frequently analyzed together due to their strong correlation. Their absolute values generally exhibit  
627 a consistent ratio of approximately 1 : 2, a relationship commonly referred to as the *Q ratio*. This ratio  
628 remains relatively stable across various saccadic amplitudes, underscoring its reliability as a metric for  
629 characterizing saccadic dynamics (Harwood et al., 1999; Garbutt et al., 2003).

630 More specifically, *saccade mean velocity* is regarded as a reliable metric for assessing the velocity  
631 of small saccades, particularly those with symmetrical velocity waveforms. The properties of saccadic  
632 velocity have been thoroughly investigated across numerous fields and clinical applications (Di Stasi et al.,  
633 2013). Early research observed that external factors such as alcohol, drugs, and fatigue lead to reductions  
634 in saccadic velocity (Dodge and Benedict, 1915; Miles, 1929), a phenomenon attributed to diminished  
635 central nervous system activation. More recently, studies have highlighted saccadic velocity as a marker  
636 for fluctuations in sympathetic nervous system activity (Di Stasi et al., 2013), variations in the intrinsic  
637 value of visual stimuli (Xu-Wilson et al., 2009), and the effects of task experience on oculomotor control  
638 (Xu-McGregor and Stern, 1996). Clinically, abnormally low saccadic velocities — commonly termed *slow*  
639 *saccades* — are symptomatic of midbrain disorders such as progressive supranuclear palsy, spinocerebellar  
640 ataxia type 2, and various cerebellar pathologies (Jensen et al., 2019).

641 While mean velocity provides a useful summary metric, it becomes less effective for saccades larger  
642 than 10 degrees, which often exhibit asymmetric velocity profiles — Figure 5b. For such larger saccades,  
643 *saccade peak velocity* is typically preferred as it reflects the highest firing rates of burst neurons driving the  
644 movement (Galley, 1989). Unlike mean velocity, peak velocity has computational advantages: it remains  
645 consistent regardless of segmentation thresholds — see Section 2 for further details — making it robust to  
646 variations in how sharply a saccade terminates during its final phase.

647 Several methodological considerations are important when calculating velocity features, particularly for  
648 saccades, though these principles extend to other canonical gaze movements as well. The simplest and most  
649 common method calculates velocity by applying a two-point central difference algorithm to the eye position  
650 signal (Schmidt et al., 1979). However, this straightforward approach has significant drawbacks. First, the  
651 numerical derivative is inherently highly sensitive to noise. Depending on the specific eye-tracking device,  
652 characterizing and removing measurement noise can be challenging or even infeasible. While filtering  
653 techniques can mitigate noise, they may inadvertently alter velocity estimates, particularly the crucial peak  
654 velocity. Second, this method is strongly influenced by sampling frequency. Since *saccade peak velocity*  
655 typically occurs between recorded samples, devices with low sampling rates often underestimate this key  
656 measure.

**Figure 5a.** Short saccade**Figure 5b.** Long saccade

**Figure 5. Saccade Velocity and Acceleration Profiles.** Examples of saccade velocity and acceleration profiles for short — Figure 5a — and long — Figure 5b — saccades, illustrating differences in peak values and overall shapes. For both types of saccades, the peak velocity is denoted as  $v_1$ , the peak acceleration as  $a_1$ , and the peak deceleration as  $a_2$ . Additionally, the duration of the acceleration phase is represented by  $t_1$ , while the duration of the deceleration phase is denoted by  $t_2$ .

657 To address these limitations, more sophisticated and robust methods have been developed. These include  
 658 the eight-point central difference derivative algorithm (Inchingolo and Spanio, 1985; Federighi et al., 2011),  
 659 which enhances noise resilience, as well as velocity profile fitting using gamma functions (Smit et al.  
 660 (1987)), and saccade trajectory curve fitting using sigmoid functions (Gibaldi and Sabatini, 2021), both  
 661 of which provide refined estimates by leveraging model-based approaches. These advanced techniques  
 662 are robust against noise and sampling artifacts, enabling accurate velocity estimation even when using

663 low-cost, low-sampling-rate eye trackers. This compatibility with accessible technologies broadens the  
664 utility of such methods for a wide range of research and practical applications.

### 665 3.2.5 Acceleration Features

666 To effectively quantify saccade acceleration characteristics, several metrics can be derived from the  
667 acceleration profile. As such, *saccade peak acceleration* is defined as the maximum absolute value of  
668 acceleration during the acceleration phase, which spans the interval from saccade onset to *saccade peak*  
669 *velocity*. Conversely, *saccade peak deceleration* represents the maximum absolute value of acceleration  
670 during the deceleration phase, occurring from peak velocity to saccade termination.

671 An additional metric of interest is the *acceleration/deceleration ratio*, computed as the ratio of the  
672 duration of the acceleration phase to that of the deceleration phase. This ratio reflects the skewness of  
673 the velocity profile. As expected, it tends to approximate one for small saccades but decreases as saccade  
674 amplitude increases. Finally, *saccade skewness* can be directly quantified through curve fitting, typically  
675 using a gamma function applied to the velocity profile. The resulting shape parameter provides a reliable  
676 estimate of skewness (Chen et al., 2002).

677 As briefly discussed in Section 3.2.4, the acceleration and deceleration characteristics of saccades vary  
678 markedly with saccade amplitude. Specifically, larger saccades exhibit left-skewed velocity profiles, where  
679 the acceleration phase constitutes roughly one-third of the total saccade duration (Baloh et al., 1975; Lin  
680 et al., 2004). This asymmetry correlates strongly with both saccade amplitude and, even more so, its  
681 duration (Van Opstal and Van Gisbergen, 1987). While the duration of the deceleration phase increases  
682 with saccade amplitude and duration, the duration of the acceleration phase remains relatively constant  
683 (Becker, 1991).

684 The asymmetry in saccade velocity profiles, as well as its relationship with saccade duration, has been  
685 consistently observed and documented over several decades. However, the physiological significance  
686 and underlying mechanisms of this phenomenon remain unclear, with no definitive hypothesis currently  
687 available in the literature. Research suggests that saccade acceleration characteristics may be subject to  
688 modification through motor learning processes (Collins et al., 2008). Furthermore, these characteristics  
689 have been linked to neurodevelopmental conditions, such as autism spectrum disorder, where abnormal  
690 acceleration and deceleration profiles have been observed (Schmitt et al., 2014). These findings highlight  
691 the potential for saccade dynamics to serve as biomarkers for both cognitive and neurological assessments.

### 692 3.2.6 Saccadic Ratios

693 Various ratios derived from saccadic characteristics have been extensively studied, revealing valuable  
694 insights into the interconnections between oculomotor mechanisms. For instance, Garbutt et al. (2003)  
695 identified abnormally high *peak velocity-to-mean velocity* ratios in saccadic trajectories recorded from  
696 patients with progressive supranuclear palsy. This anomaly suggested that these movements might not be  
697 purely saccadic but rather comprise a sequence of small-amplitude saccades.

698 In healthy individuals, saccadic ratios have been shown to reflect low-level idiosyncrasies. For example,  
699 these ratios have been employed as biometric features for individual identification among other eye-  
700 movement metrics (Rigas and Komogortsev, 2016). Extending this analysis to higher cognitive functions,  
701 Gupta and Routray (2012) demonstrated a significant correlation between the *peak velocity-to-duration*  
702 ratio and human alertness, suggesting its utility for vigilance monitoring. These findings underscore the  
703 potential of saccadic ratios as versatile markers, ranging from physiological baselines to cognitive states.

704 Shifting focus to broader measures of eye movement dynamics, the *saccade-fixation ratio*, introduced by  
705 Goldberg and Kotval (1999), highlights the balance between exploratory behavior — searching — and  
706 cognitive processing — information extraction. A higher value for this ratio reflects increased searching  
707 relative to processing. This metric has been used in comparative studies of different layouts or visual  
708 representations. Both the total *fixation-to-saccade duration* ratio and the average *fixation-to-saccade*  
709 *duration* ratio per occurrence can be derived from this measure. These simple yet powerful metrics have  
710 been employed in diverse experimental contexts to assess attention and cognitive information processing  
711 levels (Bhoir et al., 2015; Berges et al., 2023).

712 Finally, we mention the *K coefficient* introduced by Krejtz et al. (2016a, 2017). This metric has emerged  
713 as an extension of the *saccade-fixation ratio* and is inherently linked to scanpath analysis. As such, it will  
714 be described in greater detail in the corresponding article of this review series.

### 715 3.2.7 Main Sequence

716 The term *main sequence* describes a consistent relationship between three fundamental saccadic  
717 parameters: amplitude, duration, and velocity (Bahill et al., 1975). Specifically, the relationship between  
718 saccadic peak velocity and amplitude demonstrates three key trends: (i) a roughly linear increase for small  
719 saccades — up to 5–10 degrees — (ii) an inflection point between 10 and 20 degrees, and (iii) a plateau  
720 where peak velocity saturates for larger saccades (Gibaldi and Sabatini, 2021). This stereotypical behavior  
721 is thought to result from an optimization process that improves visual performance amidst internal noise and  
722 peripheral visual uncertainty (Harris and Wolpert, 2006; Saeb et al., 2011; van Opstal and Goossens, 2008).  
723 Additionally, the *main sequence* exhibits a linear relationship between saccade duration and amplitude  
724 for saccades up to approximately 80 degrees (Baloh et al., 1975), as shown in Figure 6a. However, most  
725 naturally occurring saccades are confined to a range of about 30 degrees in the absence of head movement  
726 (Lebedev et al., 1996).

727 The *main sequence* is widely employed in clinical research as a diagnostic tool to evaluate the integrity  
728 of the saccadic system. Deviations from its expected patterns and abnormalities in saccadic behavior are  
729 indicative of various neurological and ocular conditions, including palsy of extraocular muscles (Metz  
730 et al., 1970; Garbutt et al., 2003), myasthenia gravis (Yee et al., 1976), cerebellar disorders (Selhorst et al.,  
731 1976), and multiple sclerosis (Frohman et al., 2002; Bijvank et al., 2019). Recent work by Guadron et al.  
732 (2023) further highlighted the diagnostic relevance of the *main sequence* by examining patients with central  
733 and peripheral retinal defects. Their findings revealed that the characteristic relationships between saccadic  
734 parameters were most disrupted when targets were located within the subjects' blind fields. This disruption  
735 underscores the critical role of visual input in planning saccadic kinematics, reinforcing the *main sequence*  
736 as a valuable lens through which the interplay between sensory input and motor control can be assessed.

737 Despite its widespread utility, there remains no universal consensus on the best mathematical model to  
738 describe the *main sequence*, particularly the non-linear relationship between peak velocity and saccade  
739 amplitude. Early work adopted power-law models to capture the non-linear growth of peak velocity with  
740 amplitude (Yarbus and Yarbus, 1967; Baloh et al., 1975; Lebedev et al., 1996). These models have proven  
741 useful for detecting performance deficits in clinical settings (Garbutt et al., 2003). For larger saccades,  
742 15–20 degrees and beyond, where the maximum velocity saturates, exponential-based models have gained  
743 traction. First proposed by Bahill et al. (1975), these models have been extensively utilized in both research  
744 and clinical diagnostics (Ramat et al., 2007; Federighi et al., 2017) and remain popular for their accuracy  
745 and applicability in recent studies (Leigh and Zee, 2015). Alternatively, logarithmic transformations allow  
746 the main sequence to be expressed as linear for saccades within the 1–15 degree range (Bahill et al., 1975,

Feature name	Description	Reference
Duration	Given a saccade sequence, computes the duration of the sequence.	Rigas et al. (2018)
Frequency	Given a set of saccade sequences, computes the number of saccades occurring per second.	Rigas et al. (2018)
Amplitude	Given a saccade sequence, computes the distance between the starting and ending points of the sequence.	Rigas et al. (2018)
Travel distance	Given a saccade sequence, computes the sum of distances between each data sample of the sequence.	Rigas et al. (2018)
Efficiency	Given a saccade sequence, computes the ratio of saccadic amplitude over the distance traveled.	Rigas et al. (2018)
Direction	Given a saccade sequence, computes the deviation from the horizontal plane of the line connecting the start and end points of the sequence.	Foulsham et al. (2008)
Successive deviation	Given a set of saccade sequences, computes the angle formed by successive saccadic trajectories, where each saccade is modeled as a vector connecting its start and end points.	Foulsham et al. (2008)
Initial direction	Given a saccade sequence, computes the initial direction of the saccadic trajectory after a fixed number of data measures.	Ludwig and Gilchrist (2002)
Initial deviation	Given a saccade sequence, computes the angle between the overall direction determined at the endpoint of the saccade, and the initial direction after a fixed number of data measures.	Ludwig and Gilchrist (2002)
Maximum curvature	Given a saccade sequence, computes the maximum perpendicular distance from any point along the saccadic trajectory to the straight line connecting the start and end points of the saccade.	Ludwig and Gilchrist (2002)
Area curvature	Given a saccade sequence, computes the area under the curve of the sampled saccadic trajectory, relative to the straight-line distance between the saccade starting and ending points.	Ludwig and Gilchrist (2002)
Mean velocity	Given a saccade sequence, computes the mean velocity of data samples within the sequence.	Rigas et al. (2018)
Peak velocity	Given a saccade sequence, computes the peak velocity of data samples belonging to the sequence.	Rigas et al. (2018)
Acceleration profile	Given a saccade sequence, computes the mean acceleration of data sample within the sequence	Rigas et al. (2018)
Mean acceleration	Given a saccade sequence, computes the mean absolute acceleration during the acceleration phase of the saccade, measured from the start point to the timestamp of peak acceleration	Rigas et al. (2018)
Skewness exponent	Given a saccade sequence, computes the shape parameter obtained by fitting a gamma function to the sequence velocity profile	Chen et al. (2002)
Amplitude to duration ratio	Given a saccade sequence, computes the sequence amplitude over duration ratio	Rigas et al. (2018)
Peak velocity to amplitude ratio	Given a saccade sequence, computes the sequence peak velocity over amplitude ratio	Rigas et al. (2018)
Peak velocity duration ratio	Given a saccade sequence, computes the sequence peak velocity over duration ratio	Rigas et al. (2018)
Peak velocity velocity ratio	Given a saccade sequence, computes the sequence peak velocity over mean velocity ratio	Rigas et al. (2018)
Main sequence	Given a set of saccade sequences, computes slopes of the amplitude/duration curve and the log peak velocity/log amplitude curve	Bahill et al. (1975)
Latency	Given a saccade sequence and a theoretical trajectory, computes the time difference between the onset of the theoretical saccade and the start time of the corresponding saccade	Whelan (2008)
Latency quantiles	Given a set of saccade sequences and a theoretical trajectory, computes the set of saccade latencies, before evaluating quantiles of the latency distribution	Vullings (2018)
Gain	Given a saccade sequence and a theoretical trajectory, computes the ratio between saccade and target amplitudes	Holmqvist et al. (2011)

**Table 2.** Saccade-based features.

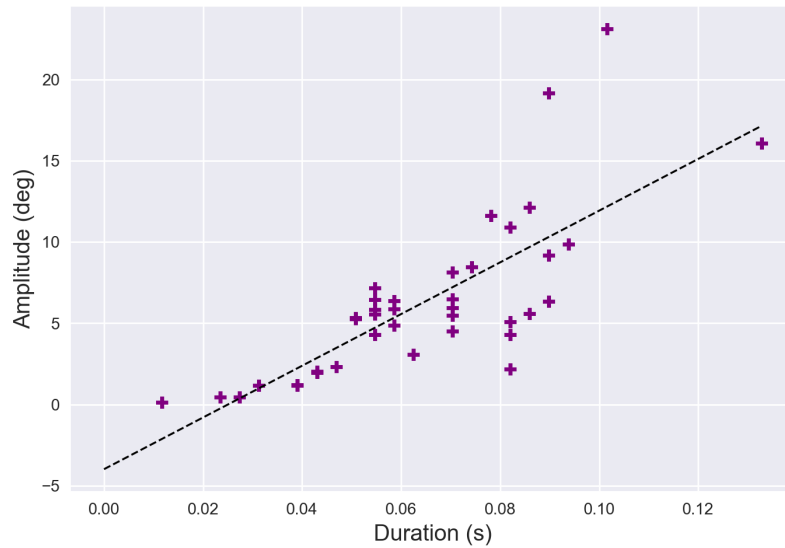


**Figure 6a.** Amplitude-duration

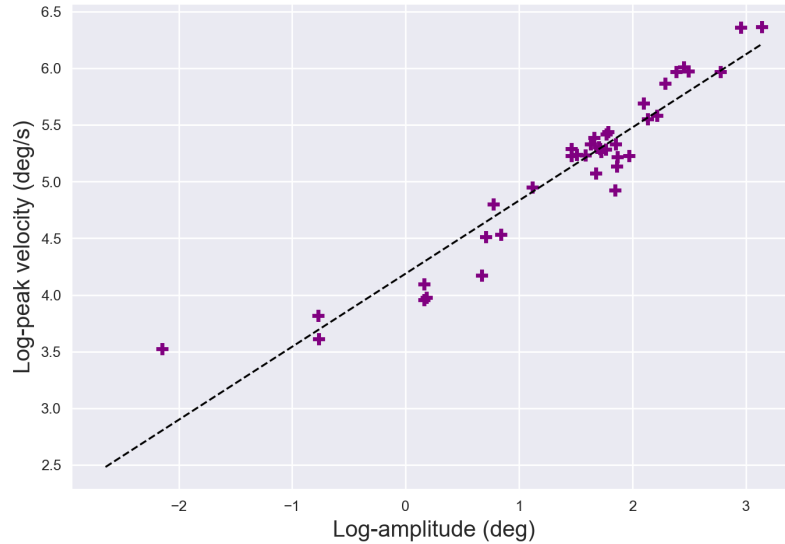


**Figure 6b.** Peak velocity-amplitude

**Figure 6. Main Sequence.** Main-sequence relationships for saccades, along with the respective linear regression fits, are shown for amplitude-duration — Figure 6a — and the logarithms of peak velocity-amplitude — Figure 6b. Each colored dot represents a saccade from a set performed by the same individual during a reading task. The data emphasize the linear relationship between the logarithms of amplitude and peak velocity for saccades of moderate amplitude. While the amplitude-duration relationship is well-established in the literature, its experimental clarity appears to be less consistent.

747 1981), as illustrated in Figure 6b. This approach simplifies analysis while preserving the relationship's  
748 fundamental trends.

749 In pursuit of greater robustness, alternative approaches have explored simpler models. For example,  
750 square-root models have been proposed to enhance the reliability of *main sequence* estimation (Lebedev  
751 et al., 1996). These models demonstrate strong generalization and repeatability, as highlighted in a recent  
752 review by Gibaldi and Sabatini (2021). Despite their simplicity, square-root models effectively capture the  
753 main sequence's three primary trends when applied to saccades larger than 1 degree — a threshold that

754 aligns with the typical amplitude range of microsaccades (Martinez-Conde et al., 2009). In conclusion,  
755 while multiple modeling approaches exist, the main sequence remains a foundational tool for understanding  
756 saccadic dynamics, with applications ranging from clinical diagnostics to explorations of the fundamental  
757 mechanisms underlying oculomotor control.

### 758 3.3 Smooth Pursuit Measures

759 Smooth pursuits represent another type of eye movement from which valuable metrics can be extracted. In  
760 natural scene viewing conditions, smooth pursuits occur alongside fixations and saccades to track moving  
761 objects within the field of view. To isolate these pursuit sequences, algorithms outlined in Section 2.2 must  
762 first be applied. In real-world scenarios, targets often move unpredictably, changing speed and direction  
763 rapidly. Such stimuli are rarely used in laboratory settings, as the performance of the smooth pursuit system  
764 is limited under these conditions, often resulting in interfering saccades that complicate the analysis.

765 In controlled experimental conditions, smooth pursuit tasks typically require the viewer to follow targets  
766 moving horizontally or vertically at a fixed frequency, back and forth. Two common types of stimuli used  
767 in these protocols are triangular and sinusoidal motion profiles. Triangular stimuli move the target at a  
768 constant velocity in one direction before abruptly reversing direction, forming a *triangle* in position-time  
769 space. This constant-velocity motion allows researchers to precisely measure the pursuit system's ability  
770 to maintain a steady eye velocity and to detect *catch-up* saccades when the eye lags behind the target. In  
771 contrast, sinusoidal stimuli move the target in a smooth, oscillating pattern where velocity continuously  
772 varies, peaking at mid-path and slowing near the reversal points. Sinusoidal motion more closely mimics  
773 naturalistic motion and tests the pursuit system's ability to adapt to continuously changing velocities. In  
774 these experimental setups, it is typically assumed that the oculomotor signal reflects primarily smooth  
775 pursuit eye movements, along with any catch-up saccades, without the inclusion of fixation sequences. The  
776 pursuit system is expected to generate smooth, coordinated eye movements that closely follow the target's  
777 trajectory, minimizing interruptions from fixational pauses.

#### 778 3.3.1 Temporal and Velocity Features

779 The analysis of smooth pursuit eye movements typically starts with the estimation of fundamental  
780 descriptors, such as *pursuit duration*, *pursuit count*, and *pursuit rate* — or *pursuit frequency*. However,  
781 interpreting these metrics is not as straightforward as it might initially appear. This complexity arises  
782 primarily from the influence of *catch-up saccades*, which are corrective eye movements that compensate  
783 for discrepancies between the target's position and the smooth pursuit response. These saccades interrupt  
784 smooth pursuit sequences, effectively shortening their duration while increasing the overall *pursuit*  
785 *frequency*.

786 More specifically, *catch-up saccades* are rapid eye movements that occur during smooth pursuit when  
787 the eye falls behind the target. They help correct the eye's position by quickly redirecting the gaze to  
788 the moving target. These saccades occur when the smooth pursuit mechanism, which is responsible for  
789 maintaining the eye's tracking of a moving object, is unable to keep up with sudden changes in the target's  
790 velocity or direction. Catch-up saccades are particularly common when the target moves too fast for the  
791 smooth pursuit system to follow continuously or during pursuit of targets with unexpected changes in  
792 velocity or direction (Boman and Hotson, 1992). Instead of maintaining a smooth motion, the eyes make  
793 these corrective jumps to *catch up* with the target, thus ensuring the target stays within the central vision.  
794 Additionally, their occurrence is modulated by factors such as target properties (Heinen et al., 2016) and  
795 clinical conditions, including schizophrenia and affective disorders (Abel et al., 1991).

796 Characterizing the velocity profile of smooth pursuit typically involves measurements of *pursuit mean*  
797 *velocity* and *pursuit peak velocity*. Smooth pursuit velocities are generally modest, ranging between 15 and  
798 30 degrees per second (Meyer et al., 1985; Zuber et al., 1968; Ettinger et al., 2003; Klein and Ettinger, 2019),  
799 significantly lower than saccadic velocities. However, trained observers or tasks involving accelerating  
800 stimuli can elicit higher peak velocities. For instance, Barmack (1970) reported peak pursuit velocities  
801 of up to 100 degrees per second during acceleration tasks. In humans, peak eye velocity typically occurs  
802 between 200 and 300 milliseconds after pursuit onset when following targets moving at velocities up to 30  
803 degrees per second (Robinson et al., 1986).

804 Importantly, the velocity profile is closely linked to temporal characteristics: as stimulus velocity increases,  
805 the frequency of *catch-up saccades* also rises to correct for larger retinal offsets. A valuable descriptor  
806 for exploring this relation between velocity and compensation mechanisms is *eye crossing time*, defined  
807 as the duration required for the eye to align with the target at constant velocity. De Brouwer et al. (2002)  
808 demonstrated that catch-up saccades are initiated when the eye crossing time reaches the saccade zone,  
809 indicating that smooth acceleration alone is insufficient for target capture.

810 However, simple spatio-temporal features such as *pursuit mean velocity* and *pursuit duration* do not  
811 fully capture the complexity of smooth pursuit dynamics. Smooth pursuit consists of two distinct phases:  
812 *open-loop* and *closed-loop*. In the open-loop phase, the eye's movement is primarily driven by the initial  
813 target presentation, with little to no influence from the retinal image changes caused by the eye movement.  
814 In contrast, during the closed-loop phase, the eye continuously adjusts to changes in the retinal image that  
815 result from its own movements, maintaining the pursuit of the target. In the following Sections 3.3.2 and  
816 3.3.3, we will introduce methods to quantify the initiation and maintenance of pursuit, respectively.

### 817 3.3.2 Smooth Pursuit Latency and Acceleration

818 In this section, we introduce two classes of features used to characterize the pursuit initiation phase,  
819 namely *pursuit latency* and *pursuit acceleration*. In target pursuit paradigms, *pursuit latency* — or *pursuit*  
820 *onset* — is commonly defined as the delay between the initiation of target motion and the start of ocular  
821 pursuit. The onset of smooth pursuit is typically calculated as the intersection point between two regression  
822 lines (Carl and Gellman, 1987). The first line represents the *pre-response baseline*, which fits the velocity  
823 signal during a time window from 100 milliseconds before target motion onset to 80 milliseconds after it  
824 begins. This baseline duration may vary depending on the experimental setup, particularly when anticipation  
825 of the target motion is expected (De Hemptinne et al., 2006). The second regression line fits the *pursuit*  
826 *initiation velocity* signal, typically recorded over a 50 milliseconds window after the pre-response baseline.  
827 This duration may differ across studies, often beginning at the first time point when eye velocity exceeds 3  
828 to 4 standard deviations of the baseline velocity measures (Krauzlis and Miles, 1996).

829 Pursuit typically exhibits much shorter latency than saccades, with *pursuit latency* ranging from 100 to  
830 125 milliseconds, compared to 200 to 250 milliseconds for saccades (Krauzlis, 2004). In experimental  
831 conditions involving anticipation, pursuit latency can be reduced to zero or even become negative, especially  
832 when pursuit begins before the target motion, such as when the direction and velocity of the stimulus are  
833 highly predictable (Burke and Barnes, 2006; De Hemptinne et al., 2006). Spering and Gegenfurtner (2007)  
834 further demonstrated that *pursuit latency* is influenced by the surrounding visual context, particularly by  
835 contrast and distracting motion orientation. They found that latency decreases when the context moves in  
836 the same direction as the target, while a rapidly moving context in the opposite direction tends to *pull* the  
837 eyes back, delaying pursuit onset. Additionally, higher contrast enhances the effect of co-linear drifting  
838 context motion, further reducing the latency before the pursuit begins.

839 In addition to latency, pursuit initiation is often examined through *pursuit initial acceleration* (Kao and  
840 Morrow, 1994). This is typically calculated as the mean second-order position derivative of the saccade-free  
841 component extracted from the tracking response within the first 100 milliseconds following pursuit onset.  
842 During this initial phase, acceleration continues until the eye velocity matches that of the target. The *pursuit*  
843 *initial peak acceleration* can also be assessed during this period. The first 20 to 30 milliseconds of eye  
844 acceleration show a modest increase with target velocity (Tychsen and Lisberger, 1986). However, between  
845 60 and 80 milliseconds after pursuit onset, eye acceleration becomes much more strongly modulated by  
846 target velocity, and is also influenced by the eccentricity of the initial eye position (Fukushima et al., 2013).

847 Furthermore, like latency, the *pursuit initial acceleration* is significantly influenced by expectations  
848 regarding the target's trajectory (Kao and Morrow, 1994). Prior knowledge of the target's movement — not  
849 only from its motion history but also from static visual cues — profoundly affects eye movements during  
850 pursuit initiation (Kao and Morrow, 1994; Ladda et al., 2007). Notably, Ladda et al. (2007) found that  
851 cue-induced acceleration during smooth pursuit increases quadratically with target velocity. This behavior  
852 aligns with the velocity scaling predicted by the *two-thirds power law*, a natural principle of biological  
853 motion (Lacquaniti et al., 1983).

### 854 3.3.3 Pursuit Gain and Accuracy

855 Smooth *pursuit gain* refers to the ratio of the eye's mean velocity to the target's mean velocity during a  
856 pursuit segment, typically under constant target velocity conditions, often referred to as *triangular stimuli*.  
857 This metric is generally assessed around 500 to 1000 milliseconds after pursuit onset, during the *pursuit*  
858 *maintenance* phase, and serves as a measure of pursuit performance. During pursuit initiation, which occurs  
859 within the first 50 to 100 milliseconds after the target starts moving, pursuit gain is primarily controlled by a  
860 visual motion (Rashbass, 1961). However, in the *pursuit maintenance* phase, the gain is influenced by a  
861 combination of visual feedback regarding performance quality and internal cues, such as anticipation and  
862 prediction of target velocity (Lencer and Trillenberg, 2008). This stable regime facilitates a more accurate  
863 assessment of performance compared to the more transient initiation phase. Typically, smooth pursuit gain  
864 is lower than 1, indicating that the eye lags behind the target, and it tends to decrease as target velocity  
865 increases (Zackon and Sharpe, 1987).

866 In sinusoidal stimulation paradigms, the smooth pursuit response is usually described by two key  
867 characteristics: *pursuit velocity phase* and *pursuit velocity gain* (Accardo et al., 1995). These values are  
868 derived by fitting the eye velocity data with a trigonometric curve for each experimental pursuit sequence.  
869 The *pursuit velocity gain* is then computed as the ratio of the peak velocity of the best-fitting curve to  
870 the peak velocity of the target's trajectory. Similarly, the *pursuit velocity phase* is computed as the phase  
871 difference between the best-fitting velocity curve and the target's velocity profile. Note that *overall gain* is  
872 also widely used in the literature, calculated as the ratio of eye velocity to target velocity (Churchland and  
873 Lisberger, 2002).

874 Smooth pursuit is often conceptualized as a negative feedback control system in which smooth eye  
875 acceleration works to eliminate retinal motion by matching the eye velocity to the target velocity.  
876 However, substantial evidence suggests that smooth pursuit gain is modulated by an *on-line* gain control  
877 mechanism, which implies distinct visual-motor gain processing during pursuit and fixation (Robinson,  
878 1965; Churchland and Lisberger, 2002). It is now widely accepted that visual inputs are not the sole  
879 mediators of smooth pursuit. Higher-order brain functions, such as attention, have been shown to play a  
880 significant role in pursuit gain and performance, though their effects have been debated (Březinová and  
881 Kendell, 1977; Acker and Toone, 1978; Kathmann et al., 1999; Van Gelder et al., 1995). Studies suggest

Feature name	Description	Reference
Duration	Given a pursuit sequence, computes the duration of the sequence	Murray et al. (2020)
Frequency	Given a set of pursuit sequences, computes the number of pursuits occurring per second	Murray et al. (2020)
Amplitude	Given a pursuit sequence, computes the distance between the starting and ending points of the sequence	Mahanama et al. (2022a)
Direction	Given a pursuit sequence, computes the deviation from the horizontal plane of the line connecting the start and end points of the sequence	Rottach et al. (1996)
Mean velocity	Given a pursuit sequence, computes the mean velocity of data sample within the sequence	Mahanama et al. (2022b)
Peak velocity	Given a pursuit sequence, computes the peak velocity of data samples	Mahanama et al. (2022b)
Latency	Given a pursuit sequence and a theoretical trajectory, computes the time difference between the onset of the theoretical smooth pursuit and the start time of the corresponding experimental pursuit	Carl and Gellman (1987)
Initial acceleration	Given a pursuit sequence and a theoretical trajectory, computes the mean second-order position derivative of the sequence in a time interval immediately following pursuit onset	Kao and Morrow (1994)
Triangular overall gain	Given a pursuit sequence and a triangular theoretical trajectory, computes the ratio between pursuit sequence and target mean velocities	Rashbass (1961)
Sinusoidal overall gain	Given a pursuit sequence and a sinusoidal theoretical trajectory, computes the ratio between pursuit sequence and target mean velocities	O'Driscoll and Callahan (2008)
Sinusoidal gain	Given a pursuit sequence and a theoretical trajectory, fits the eye velocity with a trigonometrical curve, before computing the ratio between the peak velocity of the best fitting curve over the target's peak velocity	Accardo et al. (1995)
Sinusoidal phase	Given a pursuit sequence and a theoretical trajectory, computes the difference between the phases of the best-fitting velocity curve and the target's velocity profile	Accardo et al. (1995)
Error entropy	Given a pursuit sequence and a theoretical trajectory, computes the pursuit velocity error series as the difference between the experimental pursuit velocities and theoretical stimulus velocities, before evaluating the approximate entropy of the velocity error series	Pincus et al. (1991)
Cross-correlation	Given a pursuit sequence and a theoretical trajectory, computes normalized cross-correlation between the experimental pursuit velocity and theoretical stimulus velocity signals	Rabiner (1978)

**Table 3.** Pursuit-based features.

882 that attention is crucial for pursuit performance (Van Donkelaar and Drew, 2002), but Stubbs et al. (2018)  
 883 demonstrated that while increased attentional demands do not alter smooth pursuit gain, they do improve  
 884 its consistency, as long as attention remains focused on the target.

885 Furthermore, smooth pursuit performance can be influenced by a trade-off between perceptual  
 886 discrimination and pursuit efficiency. Specifically, when a perceptual discrimination task involves objects  
 887 moving at a different velocity from the pursuit target, the ability to maintain smooth pursuit is compromised  
 888 (Khurana and Kowler, 1987). More recently, Kerzel et al. (2009) or Souto and Kerzel (2014) have  
 889 further confirmed this interdependence between target selection for pursuit and perceptual processing.  
 890 This interaction is generally understood as reflecting a shared, limited resource that is required for both  
 891 steady-state smooth pursuit and perceptual tasks (Stolte et al., 2023).

892 Finally, smooth pursuit gain has become a crucial measure in neuro-pathological research. For example,  
 893 a review by Franco et al. (2014) highlighted studies showing that individuals diagnosed with schizophrenia  
 894 often exhibit lower smooth pursuit gain. Smooth pursuit performance is also a valuable tool in assessing  
 895 sensorimotor development in preadolescence and adolescence. Horizontal smooth pursuit typically matures

896 by age 7 (Ingster-Moati et al., 2009), while vertical smooth pursuit does not reach maturity until late  
897 adolescence (Katsanis et al., 1998). This asymmetry between horizontal and vertical pursuit is due to  
898 the involvement of different brain structures in controlling these movements (Collewijn and Tamminga,  
899 1984; Grönqvist et al., 2006), with significant clinical implications. For instance, Robert et al. (2014)  
900 demonstrated that children with developmental coordination disorder often exhibit impaired vertical pursuit  
901 performance, indicating delayed maturation of the pursuit system in this population.

## 4 SIGNAL ANALYSIS

902 In this section, we review time series analysis methods for the study of ocular behavior. Compared to  
903 traditional neurophysiological approaches, these methods are underexplored but offer a robust framework  
904 for analyzing eye movements as a cohesive, dynamic system. In contrast to neurophysiological methods,  
905 which focus on specific neural circuits associated with individual eye movement types, time series  
906 approaches capture the temporal and structural patterns of eye behavior across contexts. Table 4 summarizes  
907 the metrics and algorithms discussed, describes each method and the required input formats, and provides  
908 key literature references to facilitate implementation.

### 909 4.1 Frequency Variables

910 Section 3 described methods for characterizing eye movements, focusing on spatial and temporal attributes  
911 such as fixation locations and saccade kinematics. These approaches often neglect the dynamic processes  
912 underlying these patterns. Spectral analysis provides an alternative framework by examining the frequency  
913 content of eye movement time series, revealing oscillatory patterns that reflect underlying dynamics (Stoica  
914 et al., 2005).

915 The spectral content of gaze data is commonly analyzed using the *discrete Fourier transform* (DFT),  
916 which converts the ocular signal into a frequency-domain representation (McGillem and Cooper, 1991). The  
917 DFT decomposes the signal by correlating it with sinusoids of varying frequencies, identifying dominant  
918 rhythmic components. The *power spectral density* (PSD) complements this by quantifying the amplitude  
919 of these rhythms as a function of frequency, offering insights into the signal's oscillatory structure. Welch's  
920 method (Welch, 1967), a widely adopted PSD estimation technique, segments the signal into overlapping  
921 windows, applies a window function, and averages the squared DFT magnitudes across segments. This  
922 approach balances frequency resolution and statistical reliability, yielding robust PSD estimates with  
923 reduced noise.

924 Spectral analysis also enables comparative studies of gaze data through metrics such as cross-spectral  
925 density and signal coherence, which are valuable for analyzing eye movement behavior across experimental  
926 conditions, individuals, or species (Ko et al., 2016). *Cross-spectral density* measures the frequency-specific  
927 covariance between two signals, while *signal coherence*, derived from cross-spectral density, quantifies the  
928 consistency of phase relationships, revealing synchronized rhythmic activities. For instance, Nakayama and  
929 Shimizu (2004) used cross-spectral density to demonstrate task-related differences in the coordination of  
930 horizontal and vertical eye movement components, highlighting the influence of task difficulty. Additionally,  
931 spectral analysis has been applied to compare real and synthetic gaze data, enabling evaluation of generative  
932 models. Duchowski et al. (2016) utilized spectral analysis to distinguish experimentally recorded gaze  
933 patterns from synthetic ones, advancing insights into eye movement dynamics.

---

**934 4.2 Stochastic Variables**

935 Directly comparing eye movement data is challenging due to the stochastic, or inherently random, nature  
936 of gaze signals, as discussed in Section 3. Modeling eye movements as random variables provides an  
937 alternative approach, uncovering physiological patterns through their statistical characteristics. A key tool,  
938 the *mean squared displacement* (MSD), tracks how gaze positions shift over time. In simple random walks,  
939 like Brownian motion with independent steps, the spread grows steadily. In complex cases, such as eye  
940 movements, the spread follows a power-law pattern, reflecting diverse neural and behavioral dynamics.

941 Isolated fixational eye movements, such as microsaccades and drift, are well-suited for stochastic analysis  
942 due to their structured yet random nature. Engbert and Kliegl (2004) used the MSD to reveal distinct  
943 patterns in these movements. On short time scales — tens to hundreds of milliseconds — fixational  
944 movements are persistent, following consistent directions to promote retinal shifts that prevent visual  
945 fading. On longer time scales, they become *anti-persistent*, with negatively correlated increments that  
946 facilitate maintaining gaze on the intended fixation point.

947 Detrended fluctuation analysis (DFA), another powerful method, quantifies long-term power-law  
948 correlations in non-stationary gaze data. Moshel et al. (2008) applied DFA to demonstrate that  
949 microsaccades enhance persistence more in horizontal than vertical fixational movements, suggesting  
950 distinct neural control mechanisms for these components (Sparks, 1986; Moschovakis, 1996). Beyond  
951 physiological studies, DFA has been used in functional research. For example, Wang and Cong (2015)  
952 employed DFA to investigate how professional experience shapes eye movement patterns in air traffic  
953 controllers, linking gaze dynamics to cognitive and task-related factors.

954 Finally, the MSD analysis of fixational movements exhibits oscillatory behavior over longer time scales  
955 (Herrmann et al., 2017). The displacement auto-correlation function (Dacf) complements MSD by  
956 comparing a movement's trajectory to its delayed versions, highlighting these rhythmic patterns. Such  
957 patterns suggest that drift movements are centrally controlled, potentially through time-delayed feedback  
958 mechanisms (Herrmann et al., 2017). These methods, summarized in Table 4, provide insights into the  
959 dynamic control of gaze allowing to explore additional temporal patterns.

**960 4.3 Topological Variables**

961 Recent studies have applied topological data analysis (TDA) to investigate the complex patterns of eye  
962 movement trajectories. Conventional measures, such as fixation durations or saccade amplitudes, often  
963 fail to capture the broader spatial and temporal structure of gaze patterns. Pioneering works by Kachan  
964 and Onuchin (2021) and Onuchin and Kachan (2023) addressed this limitation by using TDA to extract  
965 novel features from eye movement data, demonstrating improved performance in recognition tasks on new  
966 gaze trajectory datasets. More recently, He et al. (2025) showed that spatial-temporal topological features  
967 derived from eye-tracking data can be informative for neural disorder screening, highlighting the clinical  
968 relevance of these TDA-based representations.

969 A central tool in TDA is persistent homology, which provides a way to measure the *shape* of a dataset  
970 across multiple scales. To illustrate, consider a set of eye positions represented as points in space. Persistent  
971 homology tracks the formation and disappearance of topological features, including connected clusters of  
972 points, circular arrangements forming loops, and higher-dimensional empty regions called voids. These  
973 features are identified through a process called a filtration, in which a scale parameter gradually increases.  
974 Initially, each point is separate, but as the scale grows, points that are close to each other become connected.  
975 A topological feature is said to be *born* when it first appears, for example when two points merge into a

Feature name	Description	Reference
Periodogram	Given a raw gaze signal, estimates power spectral density	McGillem and Cooper (1991)
Welch periodogram	Given a raw gaze signal, estimates power spectral density, using a Welch windowed periodogram	Welch (1967)
Cross spectral density	Given a set of raw gaze signals, estimates the cross power spectral density between pairs of signals	McGillem and Cooper (1991)
Welch cross spectral density	Given a set of raw gaze signals, estimates the cross power spectral density between pairs of signals, according to Welch's method	McGillem and Cooper (1991)
Coherency	Given a set of raw gaze signals, estimates how strongly pairs of signals are related at specific frequencies	Bendat and Piersol (1986)
Mean squared displacement	Given a raw gaze signal, estimates the average squared deviation of the eye-gaze position from a reference position over time	Herrmann et al. (2017)
Displacement auto-correlation function	Given a raw gaze signal, estimates the degree of similarity between the gaze signal and a lagged version of itself over successive time intervals	Herrmann et al. (2017)
Detrended fluctuation analysis	Given a raw gaze signal, estimates long-range correlations and scaling behavior by analyzing signal fluctuations over different time scales	Wang and Cong (2015)
Persistence size	Given a raw gaze signal, estimates the entropy of the size of the holes in the persistence diagram obtained from gaze signal	Chung et al. (2021)
Persistence robustness	Given a raw gaze signal, estimates the entropy of the robustness of the holes in the persistence diagram obtained from gaze signal	Chung et al. (2021)
Betti curve	Given a raw gaze signal, estimates a function evaluating the Betti numbers obtained from a persistence diagram, at different levels of filtration	Güzel and Kaygun (2023)
persistence curve	Given a raw gaze signal, estimates a function that summarizes the total persistence of topological hole of the persistence diagram, at different levels of filtration	Kachan and Onuchin (2021)
Persistence entropy	Given a raw gaze signal, estimates the Shannon entropy of the collections of topological holes lifetimes of the persistence diagram obtained from gaze signal	Kachan and Onuchin (2021)

**Table 4.** Signal-based features.

cluster or a loop forms, and it *dies* when it disappears, such as when two clusters merge into one larger cluster or a loop is filled in. By recording the birth and death of each feature, the structural information of the dataset can be summarized in a persistence diagram, where longer-lived features typically represent meaningful structures while short-lived features correspond to noise (Carlsson, 2009; Edelsbrunner and Harer, 2022). Figure 7 illustrates this process schematically.

One common method to build topological structures is the Vietoris-Rips complex. In this approach, points in a cloud are connected if they are within a certain distance defined by the current scale parameter. Sets of points that are mutually connected form higher-dimensional shapes: a pair of points forms a line segment, three points form a filled triangle, and four points form a tetrahedron. As the scale increases, more connections are added, creating new features or merging existing ones. This gradual growth generates the birth and death events that are tracked in persistent homology.

Kachan and Onuchin (2021) proposed two TDA-based approaches for analyzing eye movements. In the first, eye positions are treated as a point cloud, ignoring timestamps, to capture spatial patterns. In the second, horizontal and vertical gaze coordinates are analyzed as separate time series to study temporal dynamics. From these representations, persistence diagrams are derived and transformed into compact features, such as the lifespan of topological features or their stability across scales. These features can be computed for Vietoris-Rips complexes or for sub-level set filtrations, which track the appearance and disappearance of features as the values of the data themselves vary, for example along intensity or velocity thresholds. Persistence diagrams can then be vectorized into structured formats suitable for machine

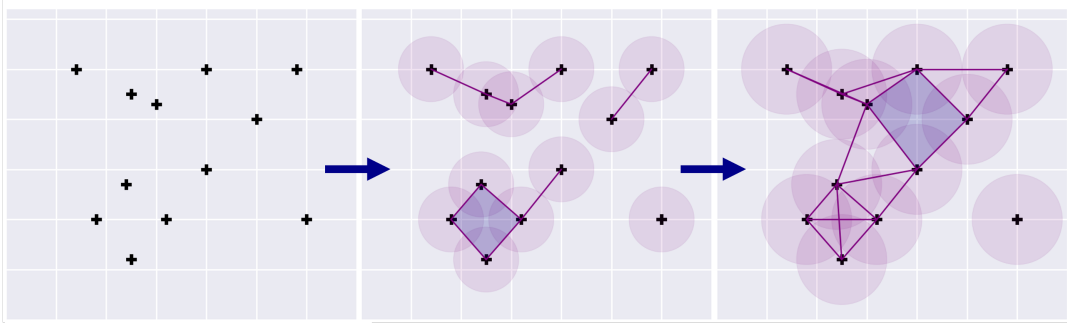


**Figure 7a.** Vietoris-Rips filtration

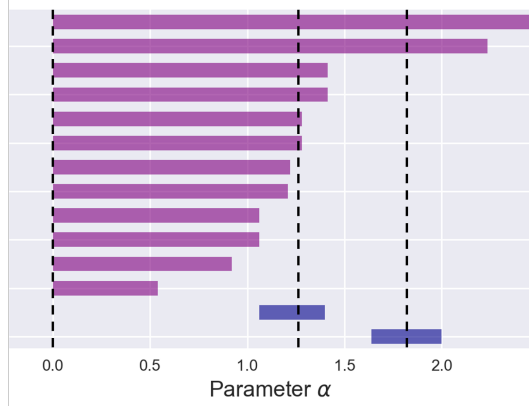


**Figure 7b.** Persistence barcode

**Figure 7. Forming Persistence Diagrams.** Given a set of points — gaze data-samples — the Vietoris-Rips filtration approximates the topology of the union of the balls of radius equal to the threshold parameter  $\alpha$  centered at each point from the dataset. The Figure 7a shows, for three values of  $\alpha$  — also represented by dotted lines in Figure 7b — appearance of topological features of dimension 0 — purple lines for connected components — and dimension 1 — blue shaded areas for holes. The persistence diagram, or persistence *barcode*, plotted Figure 7b of dimension 0 — purple bars — summarizes the linking of clusters while the persistence diagram of dimension 1 — blue bars — summarizes the number of topological holes between clusters, describing the complexity of clusters arrangement.

995 learning, enabling classification, clustering, or other data-driven analyses. By emphasizing shape-related  
 996 properties of gaze data, TDA provides tools to capture structural patterns that traditional metrics often  
 997 overlook, and as shown by He et al. (2025), these spatial-temporal topological features can also serve as  
 998 biomarkers for neural disorder screening..

## 5 DISCUSSION

999 The segmentation of raw gaze data into a sequence of oculomotor events remains a cornerstone of eye  
 1000 movement research. In this article, we have reviewed the most common segmentation algorithms — Section  
 1001 2). Historically, threshold-based methods dominated the field, relying on predefined criteria such as velocity  
 1002 or displacement thresholds to categorize eye movements. These approaches remain widely used because  
 1003 of their simplicity, computational efficiency, and relatively low barrier to implementation. However, they  
 1004 also exhibit critical limitations: their sensitivity to parameter selection can lead to inconsistent results  
 1005 across laboratories, and their robustness often degrades in noisy or dynamic environments, such as mobile

1006 or low-cost eye trackers. These drawbacks highlight the need for approaches that are less dependent on  
1007 arbitrary thresholds and more adaptable to variability in recording conditions.

1008 In contrast, learning-based approaches have gained prominence by leveraging annotated datasets that  
1009 encode expert knowledge of eye movement types. By training models on rich and diverse data, these  
1010 methods can capture complex patterns in the gaze signal that extend beyond traditional definitions of  
1011 fixations, saccades, and pursuits. For instance, they are better suited to handle ambiguous or overlapping  
1012 cases, where threshold-based approaches often fail. Nevertheless, their performance is critically dependent  
1013 on model architecture, hyperparameter optimization, and, above all, the quality, diversity, and size of the  
1014 training datasets. A model trained on limited or biased data may perform well within a narrow domain but  
1015 fail to generalize to different populations, tasks, or devices. This dependency underscores the importance  
1016 of carefully curated datasets and rigorous cross-validation protocols.

1017 To foster transparency and reproducibility in machine learning–based segmentation, detailed  
1018 methodological reporting is essential. Beyond describing the general algorithmic approach, authors should  
1019 provide explicit documentation of the algorithms and software packages employed, the hyperparameter  
1020 configurations chosen, and the strategies used for validation. Where feasible, access to training and  
1021 validation datasets should also be shared, either through open repositories or upon reasonable request. Such  
1022 openness ensures that results can be replicated, facilitates the systematic refinement of models, and lowers  
1023 the entry barrier for new research groups seeking to build upon existing work. Ultimately, transparent  
1024 reporting practices strengthen confidence in published findings and encourage convergence toward best  
1025 practices in the field.

1026 In this regard, specialized databases are playing an increasingly central role. Resources such as the  
1027 GazeBase dataset (Griffith et al., 2021) provide large and heterogeneous eye movement recordings  
1028 across diverse tasks, from controlled guided stimuli designed to elicit specific movements, to goal-  
1029 directed activities, and free-viewing scenarios such as reading or video watching. These datasets are  
1030 indispensable for benchmarking both traditional and learning-based algorithms, enabling fair comparisons  
1031 across methods, and for training models with stronger generalizability across tasks and hardware. By  
1032 facilitating standardized evaluation, such databases support the transition from isolated methodological  
1033 contributions toward a cumulative science of eye movement analysis. Looking ahead, the expansion of  
1034 open repositories covering diverse populations, age groups, and experimental contexts will be critical for  
1035 building robust segmentation algorithms with real-world applicability.

1036 Beyond segmentation itself, this article has also reviewed the metrics derived from canonical oculomotor  
1037 events — Section 3. These metrics are essential for characterizing fixations, saccades, and smooth pursuits  
1038 in terms of their temporal, spatial, and kinematic properties, and for linking them to cognitive, clinical,  
1039 and applied research contexts. For example, fixation duration can be tied to attentional processes, while  
1040 saccade amplitude and velocity are informative about motor control and neurological function. However,  
1041 meaningful cross-study comparisons are only possible if these metrics are computed in standardized  
1042 ways and interpreted within a shared conceptual framework. Advancing this line of work therefore  
1043 requires: (i) a unified set of definitions and formal concepts, (ii) standardized analytical pipelines that  
1044 minimize methodological variability, and (iii) accessible open-source datasets and software packages  
1045 that encourage reproducibility and methodological convergence. Together, these elements will harmonize  
1046 computational practices, foster interdisciplinary collaboration, and ultimately improve the comparability  
1047 and interpretability of findings across the diverse fields that rely on eye movement research.

1048 It is important to stress, however, that the robustness of segmentation and derived metrics depends  
1049 strongly on the hardware employed. High-speed laboratory-grade eye trackers — 500–1000 Hz — provide  
1050 fine-grained temporal resolution, yielding reliable estimates of fixation stability, saccade dynamics, and  
1051 pursuit gain. In these conditions, reproducibility is typically high for metrics such as RMSD or Cohen's  
1052 Kappa. By contrast, low-cost or mobile devices — 30–120 Hz — are more prone to noise and data loss,  
1053 which introduces uncertainty in event boundaries. Fixations, being relatively long in duration, are somewhat  
1054 resilient, although noise can still inflate false positives. Saccades, in turn, are especially vulnerable: low  
1055 sampling rates may miss peak velocities or misestimate onset and offset times, leading to degraded temporal  
1056 precision and event-level accuracy. These differences underscore the need for robust, hardware-agnostic  
1057 metrics that remain interpretable across diverse research settings.

1058 Looking ahead, several technological and methodological trends promise to reshape oculomotor research.  
1059 The rapid adoption of VR platforms equipped with eye tracking enables exploration of gaze behavior  
1060 in immersive, ecologically valid 3D contexts, where traditional eye movements interact with head and  
1061 body dynamics (Adhanom et al., 2023). The growing use of mobile eye tracking is similarly expanding  
1062 research far beyond lab settings, though it raises significant challenges in data quality and reproducibility  
1063 (Fu et al., 2024). On the computational front, while AI and deep learning methods for event segmentation  
1064 are emerging, the need for rigorous evaluation and privacy-aware implementations remains pressing —  
1065 especially in VR contexts (Bozkir et al., 2023). More broadly, as Extended Reality (XR) environments  
1066 integrate eye tracking with multimodal sensors, methodologies must adapt to both technological possibilities  
1067 and ethical considerations (Kourtesis, 2024). Together, these advances point toward richer, more scalable,  
1068 and context-sensitive analyses of oculomotor behavior.

1069 Finally, we reviewed emerging approaches that challenge the traditional paradigm of segmentation into  
1070 discrete events — Section 4. Advanced signal processing methods, such as topological data analysis  
1071 (TDA), enable the study of the intrinsic structure of eye movement signals without imposing predefined  
1072 categories. By focusing on patterns such as connectivity, loops, or voids in gaze trajectories, TDA captures  
1073 structural properties that may be overlooked by conventional event-based frameworks. This represents  
1074 a promising step toward more naturalistic analyses, particularly in contexts where boundaries between  
1075 fixations, saccades, and pursuits are ambiguous or functionally irrelevant. As these methods mature, they  
1076 are likely to complement existing frameworks and enrich our understanding of oculomotor control in  
1077 real-world visual behavior.

## CONFLICT OF INTEREST STATEMENT

1078 Author QL was employed by company SNCF. Author AR was employed by company Thales AVS France.  
1079 The remaining authors declare that the research was conducted in the absence of any commercial or  
1080 financial relationships that could be construed as a potential conflict of interest.

## AUTHOR CONTRIBUTIONS

1081 QL: Formal Analysis, Methodology, Writing – original draft, Writing – review & editing. AR: Formal  
1082 Analysis, Writing – original draft, Writing – review & editing. AA: Validation, Writing – review & editing.  
1083 NV: Supervision, Methodology, Validation, Writing – review & editing. IB: Supervision, Methodology,  
1084 Validation, Writing – review & editing. LO: Supervision, Methodology, Validation, Writing – review &  
1085 editing. PPV: Supervision, Methodology, Validation, Writing – review & editing.

## ACKNOWLEDGMENTS

1086 Part of this work has been founded by the Industrial Data Analytics And Machine Learning chairs of ENS  
1087 Paris-Saclay.

## REFERENCES

- 1088 Abel, L. A., Friedman, L., Jesberger, J., Malki, A., and Meltzer, H. (1991). Quantitative assessment  
1089 of smooth pursuit gain and catch-up saccades in schizophrenia and affective disorders. *Biological*  
1090 *psychiatry* 29, 1063–1072
- 1091 Accardo, A., Pensiero, S., Da Pozzo, S., and Perissutti, P. (1995). Characteristics of horizontal smooth  
1092 pursuit eye movements to sinusoidal stimulation in children of primary school age. *Vision research* 35,  
1093 539–548
- 1094 Acker, W. and Toone, B. (1978). Attention, eye tracking and schizophrenia. *British Journal of Social and*  
1095 *Clinical Psychology* 17, 173–181
- 1096 Adhanom, I. B., MacNeilage, P., and Folmer, E. (2023). Eye tracking in virtual reality: a broad review of  
1097 applications and challenges. *Virtual Reality* 27, 1481–1505
- 1098 Andersson, R., Larsson, L., Holmqvist, K., Stridh, M., and Nyström, M. (2016). One algorithm to rule  
1099 them all? an evaluation and discussion of ten eye movement event-detection algorithms. *Behavior*  
1100 *Research Methods*, 1–22
- 1101 Bahill, A., Brockenbrough, A., and Troost, B. (1981). Variability and development of a normative data  
1102 base for saccadic eye movements. *Investigative ophthalmology & visual science* 21, 116–125
- 1103 Bahill, A. T., Clark, M. R., and Stark, L. (1975). The main sequence, a tool for studying human eye  
1104 movements. *Mathematical biosciences* 24, 191–204
- 1105 Baloh, R. W., Sills, A. W., Kumley, W. E., and Honrubia, V. (1975). Quantitative measurement of saccade  
1106 amplitude, duration, and velocity. *Neurology* 25, 1065–1065
- 1107 Barmack, N. (1970). Modification of eye movements by instantaneous changes in the velocity of visual  
1108 targets. *Vision research* 10, 1431–1441
- 1109 Becker, W. (1991). Saccades. *Vision and visual dysfunction* 8, 95–137
- 1110 Bendat, J. and Piersol, A. (1986). Random data: Analysis and measurement procedures 2nd edition a  
1111 wiley-interscience publication. *New York*
- 1112 Berges, A. J., Vedula, S. S., Chara, A., Hager, G. D., Ishii, M., and Malpani, A. (2023). Eye tracking and  
1113 motion data predict endoscopic sinus surgery skill. *The Laryngoscope* 133, 500–505
- 1114 Bhoir, S. A., Hasanzadeh, S., Esmaeili, B., Dodd, M. D., and Fardhosseini, M. S. (2015). Measuring  
1115 construction workers attention using eye-tracking technology
- 1116 Bijvank, J. N., van Rijn, L., Kamminga, M., Tan, H., Uitdehaag, B., Petzold, A., et al. (2019). Saccadic  
1117 fatigability in the oculomotor system. *Journal of the neurological sciences* 402, 167–174
- 1118 Bilmes, J. A. et al. (1998). A gentle tutorial of the em algorithm and its application to parameter estimation  
1119 for gaussian mixture and hidden markov models. *International computer science institute* 4, 126
- 1120 Binkley, D., Davis, M., Lawrie, D., Maletic, J. I., Morrell, C., and Sharif, B. (2013). The impact of  
1121 identifier style on effort and comprehension. *Empirical software engineering* 18, 219–276
- 1122 Birawo, B. and Kasprowski, P. (2022). Review and evaluation of eye movement event detection algorithms.  
1123 *Sensors* 22, 8810
- 1124 Blignaut, P. (2009). Fixation identification: The optimum threshold for a dispersion algorithm. *Attention,*  
1125 *Perception, & Psychophysics* 71, 881–895
- 1126 Boman, D. K. and Hotson, J. R. (1992). Predictive smooth pursuit eye movements near abrupt changes in  
1127 motion direction. *Vision research* 32, 675–689
- 1128 Bozkir, E., Özdel, S., Wang, M., David-John, B., Gao, H., Butler, K., et al. (2023). Eye-tracked virtual  
1129 reality: A comprehensive survey on methods and privacy challenges. *arXiv preprint arXiv:2305.14080*
- 1130 Březinová, V. and Kendell, R. (1977). Smooth pursuit eye movements of schizophrenics and normal people  
1131 under stress. *The British Journal of Psychiatry* 130, 59–63

- 1132 Brunyé, T. T., Drew, T., Weaver, D. L., and Elmore, J. G. (2019). A review of eye tracking for understanding  
1133 and improving diagnostic interpretation. *Cognitive research: principles and implications* 4, 1–16
- 1134 Brysbaert, M., Vitu, F., and Schroyens, W. (1996). The right visual field advantage and the optimal viewing  
1135 position effect: On the relation between foveal and parafoveal word recognition. *Neuropsychology* 10,  
1136 385
- 1137 Burke, M. and Barnes, G. (2006). Quantitative differences in smooth pursuit and saccadic eye movements.  
1138 *Experimental brain research* 175, 596–608
- 1139 Camerini, P., Galbiati, G., and Maffioli, F. (1988). Algorithms for finding optimum trees: Description, use  
1140 and evaluation. *Annals of Operations Research* 13, 263–397
- 1141 Carl, J. and Gellman, R. (1987). Human smooth pursuit: stimulus-dependent responses. *Journal of  
1142 Neurophysiology* 57, 1446–1463
- 1143 Carlsson, G. (2009). Topology and data. *Bulletin of the American Mathematical Society* 46, 255–308
- 1144 Cerquera-Jaramillo, M. A., Nava-Mesa, M. O., González-Reyes, R. E., Tellez-Conti, C., and de-la Torre,  
1145 A. (2018). Visual features in alzheimer's disease: from basic mechanisms to clinical overview. *Neural  
1146 plasticity*
- 1147 Chen, Y.-F., Lin, H.-H., Chen, T., Tsai, T.-T., and Shee, I.-F. (2002). The peak velocity and  
1148 skewness relationship for the reflexive saccades. *Biomedical Engineering: Applications, Basis and  
1149 Communications* 14, 71–80
- 1150 Chen-Harris, H., Joiner, W. M., Ethier, V., Zee, D. S., and Shadmehr, R. (2008). Adaptive control of  
1151 saccades via internal feedback. *Journal of Neuroscience* 28, 2804–2813
- 1152 Chung, Y.-M., Hu, C.-S., Lo, Y.-L., and Wu, H.-T. (2021). A persistent homology approach to heart rate  
1153 variability analysis with an application to sleep-wake classification. *Frontiers in physiology* 12, 637684
- 1154 Churchland, A. K. and Lisberger, S. G. (2002). Gain control in human smooth-pursuit eye movements.  
1155 *Journal of Neurophysiology* 87, 2936–2945
- 1156 Collewijn, H. and Tamminga, E. P. (1984). Human smooth and saccadic eye movements during voluntary  
1157 pursuit of different target motions on different backgrounds. *The Journal of physiology* 351, 217–250
- 1158 Collins, T. and Doré-Mazars, K. (2006). Eye movement signals influence perception: evidence from the  
1159 adaptation of reactive and volitional saccades. *Vision research* 46, 3659–3673
- 1160 Collins, T., Semroud, A., Orriols, E., and Doré-Mazars, K. (2008). Saccade dynamics before, during, and  
1161 after saccadic adaptation in humans. *Investigative ophthalmology & visual science* 49, 604–612
- 1162 Crossland, M., Sims, M., Galbraith, R., and Rubin, G. (2004). Evaluation of a new quantitative technique to  
1163 assess the number and extent of preferred retinal loci in macular disease. *Vision research* 44, 1537–1546
- 1164 Crossland, M. D., Dunbar, H. M., and Rubin, G. S. (2009). Fixation stability measurement using the mp1  
1165 microperimeter. *Retina* 29, 651–656
- 1166 De Brouwer, S., Yuksel, D., Blohm, G., Missal, M., and Lefèvre, P. (2002). What triggers catch-up  
1167 saccades during visual tracking? *Journal of neurophysiology* 87, 1646–1650
- 1168 De Hemptinne, C., Lefevre, P., and Missal, M. (2006). Influence of cognitive expectation on the initiation  
1169 of anticipatory and visual pursuit eye movements in the rhesus monkey. *Journal of neurophysiology* 95,  
1170 3770–3782
- 1171 Di Stasi, L. L., Catena, A., Canas, J. J., Macknik, S. L., and Martinez-Conde, S. (2013). Saccadic velocity  
1172 as an arousal index in naturalistic tasks. *Neuroscience & Biobehavioral Reviews* 37, 968–975
- 1173 Dodge, R. and Benedict, F. G. (1915). *Psychological effects of alcohol: an experimental investigation of  
1174 the effects of moderate doses of ethyl alcohol on a related group of neuro-muscular processes in man,*  
1175 vol. 232 (Carnegie institution of Washington)
- 1176 Dodge, R. and Cline, T. S. (1901). The angle velocity of eye movements. *Psychological Review* 8, 145

- 1177 Donkelaar, P. v., Siu, K.-C., and Walterschied, J. (2004). Saccadic output is influenced by limb kinematics  
1178 during eye—hand coordination. *Journal of motor behavior* 36, 245–252
- 1179 Doyle, M. and Walker, R. (2001). Curved saccade trajectories: Voluntary and reflexive saccades curve  
1180 away from irrelevant distractors. *Experimental brain research* 139, 333–344
- 1181 Duchowski, A. T. and Duchowski, A. T. (2017). *Eye tracking methodology: Theory and practice* (Springer)
- 1182 Duchowski, A. T., Jörg, S., Allen, T. N., Giannopoulos, I., and Krejtz, K. (2016). Eye movement synthesis.  
1183 In *Proceedings of the ninth biennial ACM symposium on eye tracking research & applications*. 147–  
1184 154
- 1185 Edelsbrunner, H. and Harer, J. L. (2022). *Computational topology: an introduction* (American  
1186 Mathematical Society)
- 1187 Engbert, R. and Kliegl, R. (2004). Microsaccades keep the eyes' balance during fixation. *Psychol. Sci.* 15,  
1188 431–436
- 1189 Ester, M., Kriegel, H.-P., Sander, J., Xu, X., et al. (1996). A density-based algorithm for discovering  
1190 clusters in large spatial databases with noise. In *kdd*. vol. 96, 226–231
- 1191 Ettinger, U., Kumari, V., Crawford, T. J., Davis, R. E., Sharma, T., and Corr, P. J. (2003). Reliability of  
1192 smooth pursuit, fixation, and saccadic eye movements. *Psychophysiology* 40, 620–628
- 1193 Federighi, P., Cevenini, G., Dotti, M. T., Rosini, F., Pretegiani, E., Federico, A., et al. (2011). Differences  
1194 in saccade dynamics between spinocerebellar ataxia 2 and late-onset cerebellar ataxias. *Brain* 134,  
1195 879–891
- 1196 Federighi, P., Ramat, S., Rosini, F., Pretegiani, E., Federico, A., and Rufa, A. (2017). Characteristic eye  
1197 movements in ataxia-telangiectasia-like disorder: an explanatory hypothesis. *Frontiers in neurology* 8,  
1198 596
- 1199 Fernández, G., Mandolesi, P., Rotstein, N. P., Colombo, O., Agamennoni, O., and Politi, L. E. (2013).  
1200 Eye movement alterations during reading in patients with early alzheimer disease. *Investigative  
1201 ophthalmology & visual science* 54, 8345–8352
- 1202 Findlay, J. M. and Gilchrist, I. D. (2003). *Active vision: The psychology of looking and seeing*. 37 (Oxford  
1203 University Press)
- 1204 Fischer, B. and Weber, H. (1993). Express saccades and visual attention. *Behav. Brain Sci.* 16, 553–567
- 1205 Fletcher, W. A. and Sharpe, J. A. (1986). Saccadic eye movement dysfunction in alzheimer's disease.  
1206 *Annals of Neurology: Official Journal of the American Neurological Association and the Child  
1207 Neurology Society* 20, 464–471
- 1208 Foulsham, T., Kingstone, A., and Underwood, G. (2008). Turning the world around: Patterns in saccade  
1209 direction vary with picture orientation. *Vision research* 48, 1777–1790
- 1210 Franco, J., De Pablo, J., Gaviria, A., Sepúlveda, E., and Vilella, E. (2014). Smooth pursuit eye movements  
1211 and schizophrenia: Literature review. *Archivos de la Sociedad Española de Oftalmología (English  
1212 Edition)* 89, 361–367
- 1213 Fried, M., Tsitsiashvili, E., Bonneh, Y. S., Sterkin, A., Wygnanski-Jaffe, T., Epstein, T., et al. (2014). Adhd  
1214 subjects fail to suppress eye blinks and microsaccades while anticipating visual stimuli but recover with  
1215 medication. *Vision research* 101, 62–72
- 1216 Frohman, E., Frohman, T., O'suilleabhain, P., Zhang, H., Hawker, K., Racke, M., et al. (2002). Quantitative  
1217 oculographic characterisation of internuclear ophthalmoparesis in multiple sclerosis: the versional  
1218 dysconjugacy index z score. *Journal of Neurology, Neurosurgery & Psychiatry* 73, 51–55
- 1219 Fu, X., Franchak, J. M., MacNeill, L. A., Gunther, K. E., Borjon, J. I., Yurkovic-Harding, J., et al. (2024).  
1220 Implementing mobile eye tracking in psychological research: A practical guide. *Behavior Research  
1221 Methods* 56, 8269–8288

- 1222 Fuhl, W., Castner, N., and Kasneci, E. (2018). Histogram of oriented velocities for eye movement detection.  
1223 In *Proceedings of the Workshop on Modeling Cognitive Processes from Multimodal Data*. 1–6
- 1224 Fuhl, W., Rong, Y., and Kasneci, E. (2021). Fully convolutional neural networks for raw eye tracking  
1225 data segmentation, generation, and reconstruction. In *2020 25th International Conference on Pattern  
1226 Recognition (ICPR)* (IEEE), 142–149
- 1227 Fukushima, K., Fukushima, J., Warabi, T., and Barnes, G. R. (2013). Cognitive processes involved in  
1228 smooth pursuit eye movements: behavioral evidence, neural substrate and clinical correlation. *Frontiers  
1229 in systems neuroscience* 7, 4
- 1230 Galley, N. (1989). Saccadic eye movement velocity as an indicator of (de) activation. a review and some  
1231 speculations
- 1232 Garbutt, S., Harwood, M. R., Kumar, A. N., Han, Y. H., and Leigh, R. J. (2003). Evaluating small eye  
1233 movements in patients with saccadic palsies. *Annals of the New York Academy of Sciences* 1004,  
1234 337–346
- 1235 Ghasia, F. and Wang, J. (2022). Amblyopia and fixation eye movements. *Journal of the Neurological  
1236 Sciences*, 120373
- 1237 Gibaldi, A. and Sabatini, S. P. (2021). The saccade main sequence revised: A fast and repeatable tool for  
1238 oculomotor analysis. *Behavior Research Methods* 53, 167–187
- 1239 Goldberg, J. H. and Kotval, X. P. (1999). Computer interface evaluation using eye movements: methods  
1240 and constructs. *International journal of industrial ergonomics* 24, 631–645
- 1241 Goldberg, J. H. and Schryver, J. C. (1995). Eye-gaze-contingent control of the computer interface:  
1242 Methodology and example for zoom detection. *Behavior research methods, instruments, & computers*  
1243 27, 338–350
- 1244 Golla, H., Tziridis, K., Haarmeier, T., Catz, N., Barash, S., and Thier, P. (2008). Reduced saccadic  
1245 resilience and impaired saccadic adaptation due to cerebellar disease. *European Journal of Neuroscience*  
1246 27, 132–144
- 1247 Griffith, H., Lohr, D., Abdulin, E., and Komogortsev, O. (2021). Gazebase, a large-scale, multi-stimulus,  
1248 longitudinal eye movement dataset. *Scientific Data* 8, 184
- 1249 Grönqvist, H., Gredebäck, G., and von Hofsten, C. (2006). Developmental asymmetries between horizontal  
1250 and vertical tracking. *Vision Research* 46, 1754–1761
- 1251 Guadron, L., Titchener, S. A., Abbott, C. J., Ayton, L. N., van Opstal, J., Petoe, M. A., et al. (2023).  
1252 The saccade main sequence in patients with retinitis pigmentosa and advanced age-related macular  
1253 degeneration. *Investigative Ophthalmology & Visual Science* 64, 1–1
- 1254 Gupta, S. and Routray, A. (2012). Estimation of saccadic ratio from eye image sequences to detect human  
1255 alertness. In *2012 4th International Conference on Intelligent Human Computer Interaction (IHCI)*  
1256 (IEEE), 1–6
- 1257 Güzel, İ. and Kaygun, A. (2023). Classification of stochastic processes with topological data analysis.  
1258 *Concurrency and Computation: Practice and Experience* 35, e7732
- 1259 Harris, C. M. and Wolpert, D. M. (2006). The main sequence of saccades optimizes speed-accuracy  
1260 trade-off. *Biological cybernetics* 95, 21–29
- 1261 Harwood, M. R., Mezey, L. E., and Harris, C. M. (1999). The spectral main sequence of human saccades.  
1262 *Journal of Neuroscience* 19, 9098–9106
- 1263 Hayhoe, M. and Ballard, D. (2005). Eye movements in natural behavior. *Trends in cognitive sciences* 9,  
1264 188–194

- 1265 He, D., Wang, S., and Ogmen, H. (2025). Spatial-temporal topological features in eye tracking data  
1266 are informative for neural disorder screening. *Investigative Ophthalmology & Visual Science* 66,  
1267 3893–3893
- 1268 Heinen, S. J., Potapchuk, E., and Watamaniuk, S. N. (2016). A foveal target increases catch-up saccade  
1269 frequency during smooth pursuit. *Journal of neurophysiology* 115, 1220–1227
- 1270 Henderson, J. M. (2003). Human gaze control during real-world scene perception. *Trends in cognitive  
1271 sciences* 7, 498–504
- 1272 Herrmann, C. J., Metzler, R., and Engbert, R. (2017). A self-avoiding walk with neural delays as a model  
1273 of fixational eye movements. *Scientific reports* 7, 1–17
- 1274 Hessels, R. S., Niehorster, D. C., Kemner, C., and Hooge, I. T. (2017). Noise-robust fixation detection  
1275 in eye movement data: Identification by two-means clustering (i2mc). *Behavior research methods* 49,  
1276 1802–1823
- 1277 Hessels, R. S., Niehorster, D. C., Nyström, M., Andersson, R., and Hooge, I. T. (2018). Is the eye-  
1278 movement field confused about fixations and saccades? a survey among 124 researchers. *Royal Society  
1279 open science* 5, 180502
- 1280 Holmqvist, K., Nystrom, M., Andersson, R., Dewhurst, R., Jarodzka, H., and Van de Weijer, J. (2011). Eye  
1281 tracking: A comprehensive guide to methods and measures. *OUP Oxford*
- 1282 Hoppe, S. and Bulling, A. (2016). End-to-end eye movement detection using convolutional neural networks.  
1283 *arXiv preprint arXiv:1609.02452*
- 1284 Hsiao, J. H.-w. and Cottrell, G. (2008). Two fixations suffice in face recognition. *Psychological science*  
1285 19, 998–1006
- 1286 Inchalingolo, P. and Spanio, M. (1985). On the identification and analysis of saccadic eye movements-  
1287 a quantitative study of the processing procedures. *IEEE Transactions on Biomedical Engineering* ,  
1288 683–695
- 1289 Ingster-Moati, I., Vaivre-Douret, L., Quoc, E. B., Albuison, E., Dufier, J.-L., and Golse, B. (2009). Vertical  
1290 and horizontal smooth pursuit eye movements in children: a neuro-developmental study. *european  
1291 journal of paediatric neurology* 13, 362–366
- 1292 Inhoff, A. W. and Radach, R. (1998). Definition and computation of oculomotor measures in the study of  
1293 cognitive processes. *Eye guidance in reading and scene perception* , 29–53
- 1294 Inhoff, A. W., Radach, R., Starr, M., and Greenberg, S. (2000). Allocation of visuo-spatial attention and  
1295 saccade programming during reading. In *Reading as a perceptual process* (Elsevier). 221–246
- 1296 Jacob, R. J. and Karn, K. S. (2003). Eye tracking in human-computer interaction and usability research:  
1297 Ready to deliver the promises. In *The mind's eye* (Elsevier). 573–605
- 1298 Jensen, K., Beylgergil, S. B., and Shaikh, A. G. (2019). Slow saccades in cerebellar disease. *Cerebellum &  
1299 Ataxias* 6, 1–9
- 1300 Kachan, O. and Onuchin, A. (2021). Topological data analysis of eye movements. *IEEE 18th International  
1301 Symposium on Biomedical Imaging*
- 1302 Kao, G. W. and Morrow, M. J. (1994). The relationship of anticipatory smooth eye movement to smooth  
1303 pursuit initiation. *Vision research* 34, 3027–3036
- 1304 Kasneci, E., Kasneci, G., Kübler, T. C., and Rosenstiel, W. (2015). Online recognition of fixations,  
1305 saccades, and smooth pursuits for automated analysis of traffic hazard perception. In *Artificial Neural  
1306 Networks: Methods and Applications in Bio-/Neuroinformatics* (Springer), 411–434
- 1307 Kathmann, N., Hochrein, A., and Uwer, R. (1999). Effects of dual task demands on the accuracy of smooth  
1308 pursuit eye movements. *Psychophysiology* 36, 158–163

- 1309 Katsanis, J., Iacono, W. G., and Harris, M. (1998). Development of oculomotor functioning in  
1310 preadolescence, adolescence, and adulthood. *Psychophysiology* 35, 64–72
- 1311 Kerzel, D., Born, S., and Souto, D. (2009). Smooth pursuit eye movements and perception share target  
1312 selection, but only some central resources. *Behavioural brain research* 201, 66–73
- 1313 Khurana, B. and Kowler, E. (1987). Shared attentional control of smooth eye movement and perception.  
1314 *Vision research* 27, 1603–1618
- 1315 Klein, C. and Ettinger, U. (2019). *Eye movement research: An introduction to its scientific foundations  
1316 and applications* (Springer Nature)
- 1317 Klin, A., Jones, W., Schultz, R., Volkmar, F., and Cohen, D. (2002). Visual fixation patterns during viewing  
1318 of naturalistic social situations as predictors of social competence in individuals with autism. *Archives  
1319 of general psychiatry* 59, 809–816
- 1320 Ko, H.-k., Snodderly, D. M., and Poletti, M. (2016). Eye movements between saccades: Measuring ocular  
1321 drift and tremor. *Vision research* 122, 93–104
- 1322 Komogortsev, O. V., Gobert, D. V., Jayarathna, S., Gowda, S. M., et al. (2010a). Standardization of  
1323 automated analyses of oculomotor fixation and saccadic behaviors. *IEEE Transactions on biomedical  
1324 engineering* 57, 2635–2645
- 1325 Komogortsev, O. V., Jayarathna, S., Koh, D. H., and Gowda, S. M. (2010b). Qualitative and quantitative  
1326 scoring and evaluation of the eye movement classification algorithms. In *Proceedings of the 2010  
1327 Symposium on eye-tracking research & applications*. 65–68
- 1328 Komogortsev, O. V. and Karpov, A. (2013). Automated classification and scoring of smooth pursuit eye  
1329 movements in the presence of fixations and saccades. *Behavior research methods* 45, 203–215
- 1330 Komogortsev, O. V. and Khan, J. I. (2007). Kalman filtering in the design of eye-gaze-guided computer  
1331 interfaces. In *International Conference on Human-Computer Interaction* (Springer), 679–689
- 1332 Kourtesis, P. (2024). A comprehensive review of multimodal xr applications, risks, and ethical challenges  
1333 in the metaverse. *Multimodal Technologies and Interaction* 8, 98
- 1334 Krauzlis, R. and Miles, F. (1996). Decreases in the latency of smooth pursuit and saccadic eye movements  
1335 produced by the “gap paradigm” in the monkey. *Vision research* 36, 1973–1985
- 1336 Krauzlis, R. J. (2004). Recasting the smooth pursuit eye movement system. *Journal of neurophysiology*  
1337 91, 591–603
- 1338 Krejtz, K., Çöltekin, A., Duchowski, A., and Niedzielska, A. (2017). Using coefficient to distinguish  
1339 ambient/focal visual attention during cartographic tasks. *Journal of eye movement research* 10
- 1340 Krejtz, K., Duchowski, A., Krejtz, I., Szarkowska, A., and Kopacz, A. (2016a). Discerning ambient/focal  
1341 attention with coefficient k. *ACM Transactions on Applied Perception (TAP)* 13, 1–20
- 1342 Krejtz, K., Duchowski, A. T., Krejtz, I., Kopacz, A., and Chrzastowski-Wachtel, P. (2016b). Gaze  
1343 transitions when learning with multimedia. *Journal of Eye Movement Research* 9
- 1344 Laborde, Q., Roques, A., Robert, M. P., Armougum, A., Vayatis, N., Bargiotas, I., et al. (2025). Vision  
1345 toolkit part 1. neurophysiological foundations and experimental paradigms in eye-tracking research: a  
1346 review. *Frontiers in Physiology* Volume 16 - 2025. doi:10.3389/fphys.2025.1571534
- 1347 Lacquaniti, F., Terzuolo, C., and Viviani, P. (1983). The law relating the kinematic and figural aspects of  
1348 drawing movements. *Acta psychologica* 54, 115–130
- 1349 Ladda, J., Eggert, T., Glasauer, S., and Straube, A. (2007). Velocity scaling of cue-induced smooth pursuit  
1350 acceleration obeys constraints of natural motion. *Experimental brain research* 182, 343–356
- 1351 Land, M. F. (2009). Vision, eye movements, and natural behavior. *Visual neuroscience* 26, 51–62
- 1352 Lebedev, S., Van Gelder, P., and Tsui, W. H. (1996). Square-root relations between main saccadic  
1353 parameters. *Investigative Ophthalmology & Visual Science* 37, 2750–2758

- 1354 Leech, J., Gresty, M., Hess, K., and Rudge, P. (1977). Gaze failure, drifting eye movements, and centripetal  
1355 nystagmus in cerebellar disease. *British Journal of Ophthalmology* 61, 774–781
- 1356 Leigh, R. J. and Zee, D. S. (2015). *The neurology of eye movements* (Contemporary Neurology)
- 1357 Lencer, R. and Trillenberg, P. (2008). Neurophysiology and neuroanatomy of smooth pursuit in humans.  
1358 *Brain and cognition* 68, 219–228
- 1359 Leonard, B., Zhang, M., Snyder, V., Holland, C., Bensinger, E., Sheehy, C. K., et al. (2019). Fixational eye  
1360 movements following concussion. *Investigative Ophthalmology & Visual Science* 60, 1035–1035
- 1361 Li, B., Wang, Q., Barney, E., Hart, L., Wall, C., Chawarska, K., et al. (2016). Modified dbscan algorithm  
1362 on oculomotor fixation identification. In *Proceedings of the Ninth Biennial ACM Symposium on Eye  
1363 Tracking Research and Applications* (New York, NY, USA: Association for Computing Machinery),  
1364 ETRA '16, 337–338. doi:10.1145/2857491.2888587
- 1365 Lin, H.-H., Chen, Y.-F., Chen, T., Tsai, T.-T., and Huang, K.-H. (2004). Temporal analysis of the  
1366 acceleration and deceleration phases for visual saccades. *Biomedical Engineering: Applications,  
1367 Basis and Communications* 16, 355–362
- 1368 Liu, H.-C. and Chuang, H.-H. (2011). An examination of cognitive processing of multimedia information  
1369 based on viewers' eye movements. *Interactive Learning Environments* 19, 503–517
- 1370 Liu, J.-C., Li, K.-A., Yeh, S.-L., and Chien, S.-Y. (2022). Assessing perceptual load and cognitive load by  
1371 fixation-related information of eye movements. *Sensors* 22, 1187
- 1372 Liu, P.-L. (2014). Using eye tracking to understand learners' reading process through the concept-mapping  
1373 learning strategy. *Computers & Education* 78, 237–249
- 1374 Liversedge, S., Gilchrist, I., and Everling, S. (2011). *The Oxford handbook of eye movements* (OUP  
1375 Oxford)
- 1376 Lopez, J. S. A. (2009). *Off-the-shelf gaze interaction*. Ph.D. thesis, Citeseer
- 1377 Ludwig, C. J. and Gilchrist, I. D. (2002). Measuring saccade curvature: A curve-fitting approach. *Behavior  
1378 Research Methods, Instruments, & Computers* 34, 618–624
- 1379 MacAskill, M. R. and Anderson, T. J. (2016). Eye movements in neurodegenerative diseases. *Current  
1380 opinion in neurology* 29, 61–68
- 1381 MacAskill, M. R., Anderson, T. J., and Jones, R. D. (2002). Adaptive modification of saccade amplitude in  
1382 parkinson's disease. *Brain* 125, 1570–1582
- 1383 Mahanama, B., Jayawardana, Y., Rengarajan, S., Jayawardena, G., Chukoskie, L., Snider, J., et al. (2022a).  
1384 Eye movement and pupil measures: A review. *Frontiers in Computer Science* 3, 733531
- 1385 Mahanama, B., Jayawardana, Y., Rengarajan, S., Jayawardena, G., Chukoskie, L., Snider, J., et al. (2022b).  
1386 Eye movement and pupil measures: A review. *Frontiers in Computer Science* 3, 733531
- 1387 Martinez-Conde, S., Macknik, S. L., Troncoso, X. G., and Hubel, D. H. (2009). Microsaccades: a  
1388 neurophysiological analysis. *Trends in neurosciences* 32, 463–475
- 1389 May, J. G., Kennedy, R. S., Williams, M. C., Dunlap, W. P., and Brannan, J. R. (1990). Eye movement  
1390 indices of mental workload. *Acta psychologica* 75, 75–89
- 1391 McGillem, C. D. and Cooper, G. R. (1991). Continuous and discrete signal and system analysis. *(No  
1392 Title)*
- 1393 McPeek, R. M., Han, J. H., and Keller, E. L. (2003). Competition between saccade goals in the superior  
1394 colliculus produces saccade curvature. *Journal of neurophysiology* 89, 2577–2590
- 1395 Megaw, E. D. and Richardson, J. (1979). Eye movements and industrial inspection. *Appl. Ergon.* 10,  
1396 145–154
- 1397 Metz, H. S., Scott, A. B., O'Meara, D., and Stewart, H. L. (1970). Ocular saccades in lateral rectus palsy.  
1398 *Archives of Ophthalmology* 84, 453–460

- 1399 Meyer, C. H., Lasker, A. G., and Robinson, D. A. (1985). The upper limit of human smooth pursuit  
1400 velocity. *Vision research* 25, 561–563
- 1401 Michell, A., Xu, Z., Fritz, D., Lewis, S., Foltynie, T., Williams-Gray, C., et al. (2006). Saccadic latency  
1402 distributions in parkinson's disease and the effects of l-dopa. *Experimental brain research* 174, 7–18
- 1403 Miles, W. R. (1929). Horizontal eye movements at the onset of sleep. *Psychological Review* 36, 122
- 1404 Montesano, G., Crabb, D. P., Jones, P. R., Fogagnolo, P., Digiuni, M., and Rossetti, L. M. (2018). Evidence  
1405 for alterations in fixational eye movements in glaucoma. *BMC ophthalmology* 18, 1–8
- 1406 Moschovakis, A. K. (1996). The superior colliculus and eye movement control. *Current opinion in*  
1407 *neurobiology* 6, 811–816
- 1408 Moshel, S., Zivotofsky, A. Z., Liang, J. R., Engbert, R., Kurths, J., and Kliegl, R. e. a. (2008). Persistence  
1409 and phase synchronisation properties of fixational eye movements. *European Physical Journal Special*  
1410 *Topics* 161, 207–223
- 1411 Mozaffari, S., Al-Naser, M., Klein, P., Küchemann, S., Kuhn, J., Widmann, T., et al. (2020). Classification  
1412 of visual strategies in physics vector field problem-solving. *ICAART (2) 2020*, 257–267
- 1413 Murray, N. G., Szekely, B., Islas, A., Munkasy, B., Gore, R., Berryhill, M., et al. (2020). Smooth pursuit  
1414 and saccades after sport-related concussion. *Journal of neurotrauma* 37, 340–346
- 1415 Nakayama, M. and Shimizu, Y. (2004). Frequency analysis of task evoked pupillary response and  
1416 eye-movement. In *Proceedings of the 2004 symposium on Eye tracking research & applications*. 71–76
- 1417 Nakayama, M., Takahashi, K., and Shimizu, Y. (2002). The act of task difficulty and eye-movement  
1418 frequency for the oculo-motor indices. *Proceedings of the 2002 symposium on Eye tracking research &*  
1419 *applications*, 37–42
- 1420 Nazir, T. A., Jacobs, A. M., and O'Regan, J. K. (1998). Letter legibility and visual word recognition.  
1421 *Memory & cognition* 26, 810–821
- 1422 Nyström, M. and Holmqvist, K. (2010). An adaptive algorithm for fixation, saccade, and glissade detection  
1423 in eyetracking data. *Behavior research methods* 42, 188–204
- 1424 Nyström, M. and Holmqvist, K. (2010). An adaptive algorithm for fixation, saccade, and glissade detection  
1425 in eyetracking data. *Behavior Research Methods* 42, 188–204
- 1426 Onuchin, A. and Kachan, O. (2023). Individual topology structure of eye movement trajectories. In  
1427 *International Conference on Neuroinformatics* (Springer), 45–55
- 1428 O'Regan, J. K. and Jacobs, A. M. (1992). Optimal viewing position effect in word recognition: A challenge  
1429 to current theory. *Journal of Experimental Psychology: Human Perception and Performance* 18, 185
- 1430 O'Driscoll, G. A. and Callahan, B. L. (2008). Smooth pursuit in schizophrenia: a meta-analytic review of  
1431 research since 1993. *Brain and cognition* 68, 359–370
- 1432 Park, B., Korbach, A., and Brünken, R. (2015). Do learner characteristics moderate the seductive-details-  
1433 effect? a cognitive-load-study using eye-tracking. *Journal of Educational Technology & Society* 18,  
1434 24–36
- 1435 Peterson, M. F. and Eckstein, M. P. (2012). Looking just below the eyes is optimal across face recognition  
1436 tasks. *Proceedings of the National Academy of Sciences* 109, E3314–E3323
- 1437 Phillips, M. H. and Edelman, J. A. (2008). The dependence of visual scanning performance on search  
1438 direction and difficulty. *Vision research* 48, 2184–2192
- 1439 Pincus, S., Gladstone, I., and Ehrenkranz, R. (1991). A regularity statistic for medical data analysis.  
1440 *Journal of Clinical Monitoring and Computing* 7, 335–345
- 1441 Rabiner, L. R. (1978). *Digital processing of speech signals* (Pearson Education India)
- 1442 Ramat, S., Leigh, R. J., Zee, D. S., and Optican, L. M. (2007). What clinical disorders tell us about the  
1443 neural control of saccadic eye movements. *Brain* 130, 10–35

- 1444 Raney, G. E., Campbell, S. J., and Bovee, J. C. (2014). Using eye movements to evaluate the cognitive  
1445 processes involved in text comprehension. *JoVE (Journal of Visualized Experiments)*, e50780
- 1446 Rashbass, C. (1961). The relationship between saccadic and smooth tracking eye movements. *The Journal  
1447 of physiology* 159, 326
- 1448 Rayner, K. (1998a). Eye movements in reading and information processing: 20 years of research.  
1449 *Psychological bulletin* 124, 372
- 1450 Rayner, K. (1998b). Eye movements in reading and information processing: 20 years of research.  
1451 *Psychological bulletin* 124, 372
- 1452 Rayner, K., Pollatsek, A., Ashby, J., and Clifton Jr, C. (2012). *Psychology of reading* (Psychology Press)
- 1453 Rigas, I., Friedman, L., and Komogortsev, O. (2018). Study of an extensive set of eye movement features:  
1454 Extraction methods and statistical analysis. *Journal of Eye Movement Research* 11
- 1455 Rigas, I. and Komogortsev, O. (2016). Biometric recognition via eye movements: Saccadic vigor and  
1456 acceleration cues. *ACM Trans. Appl. Percept.*
- 1457 Ritchie, L. (1976). Effects of cerebellar lesions on saccadic eye movements. *Journal of neurophysiology*  
1458 39, 1246–1256
- 1459 Robert, M. P., Ingster-Moati, I., Albuisson, E., Cabrol, D., Golse, B., and Vaivre-Douret, L. (2014). Vertical  
1460 and horizontal smooth pursuit eye movements in children with developmental coordination disorder.  
1461 *Developmental Medicine & Child Neurology* 56, 595–600
- 1462 Robinson, D. A. (1965). The mechanics of human smooth pursuit eye movement. *The Journal of  
1463 Physiology* 180, 569
- 1464 Robinson, D. A., Gordon, J., and Gordon, S. (1986). A model of the smooth pursuit eye movement system.  
1465 *Biological cybernetics* 55, 43–57
- 1466 Rottach, K. G., Zivotofsky, A. Z., Das, V. E., Averbuch-Heller, L., Discenna, A. O., Poonyathalang, A.,  
1467 et al. (1996). Comparison of horizontal, vertical and diagonal smooth pursuit eye movements in normal  
1468 human subjects. *Vision research* 36, 2189–2195
- 1469 Saeb, S., Weber, C., and Triesch, J. (2011). Learning the optimal control of coordinated eye and head  
1470 movements. *PLoS computational biology* 7, e1002253
- 1471 Salvucci, D. D. and Goldberg, J. H. (2000). Identifying fixations and saccades in eye-tracking protocols.  
1472 In *Proceedings of the 2000 Symposium on Eye Tracking Research and Applications* (New York, NY,  
1473 USA: Association for Computing Machinery), ETRA '00, 71–78. doi:10.1145/355017.355028
- 1474 Santini, T., Fuhl, W., Kübler, T., and Kasneci, E. (2016). Bayesian identification of fixations, saccades, and  
1475 smooth pursuits. In *Proceedings of the Ninth Biennial ACM Symposium on Eye Tracking Research &  
1476 Applications*. 163–170
- 1477 Sauter, D., Martin, B., Di Renzo, N., and Vomscheid, C. (1991). Analysis of eye tracking movements  
1478 using innovations generated by a kalman filter. *Medical and biological Engineering and Computing* 29,  
1479 63–69
- 1480 Scheiter, K. and Eitel, A. (2017). The use of eye tracking as a research and instructional tool in multimedia  
1481 learning. In *Eye-tracking technology applications in educational research* (IGI Global). 143–164
- 1482 Schmidt, D., Abel, L., DellOsso, L., and Daroff, R. (1979). Saccadic velocity characteristics- intrinsic  
1483 variability and fatigue. *Aviation, space, and environmental medicine* 50, 393–395
- 1484 Schmitt, L. M., Cook, E. H., Sweeney, J. A., and Mosconi, M. W. (2014). Saccadic eye movement  
1485 abnormalities in autism spectrum disorder indicate dysfunctions in cerebellum and brainstem. *Molecular  
1486 autism* 5, 1–13
- 1487 Schoonahd, J. W., Gould, J. D., and Miller, L. A. (1973). Studies of visual inspection. *Ergonomics* 16,  
1488 365–379

- 1489 Schor, C. M. and Westall, C. (1984). Visual and vestibular sources of fixation instability in amblyopia.  
1490 *Investigative ophthalmology & visual science* 25, 729–738
- 1491 Schütz, A. C., Braun, D. I., and Gegenfurtner, K. R. (2011). Eye movements and perception: A selective  
1492 review. *Journal of vision* 11, 9–9
- 1493 Selhorst, J. B., Stark, L., Ochs, A. L., and Hoyt, W. F. (1976). Disorders in cerebellar ocular motor control.  
1494 i. saccadic overshoot dysmetria. an oculographic, control system and clinico-anatomical analysis. *Brain: a journal of neurology* 99, 497–508
- 1495 Shaikh, A. G., Otero-Millan, J., Kumar, P., and Ghasia, F. F. (2016). Abnormal fixational eye movements  
1496 in amblyopia. *PLoS one* 11, e0149953
- 1497 Sharafi, Z., Shaffer, T., Sharif, B., and Guéhéneuc, Y.-G. (2015). Eye-tracking metrics in software  
1498 engineering. In *2015 Asia-Pacific Software Engineering Conference (APSEC)* (IEEE), 96–103
- 1499 Sharif, B., Falcone, M., and Maletic, J. I. (2012). An eye-tracking study on the role of scan time in finding  
1500 source code defects. In *Proceedings of the Symposium on Eye Tracking Research and Applications*.  
1501 381–384
- 1502 Sheliga, B., Craighero, L., Riggio, L., and Rizzolatti, G. (1997). Effects of spatial attention on directional  
1503 manual and ocular responses. *Experimental brain research* 114, 339–351
- 1504 Sheliga, B. M., Riggio, L., Craighero, L., and Rizzolatti, G. (1995). Spatial attention-determined  
1505 modifications in saccade trajectories. *Neuroreport: An International Journal for the Rapid  
1506 Communication of Research in Neuroscience*
- 1507 Shic, F., Scassellati, B., and Chawarska, K. (2008). The incomplete fixation measure. In *Proceedings of  
1508 the 2008 symposium on Eye tracking research & applications*. 111–114
- 1509 Shirama, A., Kanai, C., Kato, N., and Kashino, M. (2016). Ocular fixation abnormality in patients with  
1510 autism spectrum disorder. *Journal of Autism and Developmental Disorders* 46, 1613–1622
- 1511 Skaramagkas, V., Giannakakis, G., Ktistakis, E., Manousos, D., Karatzanis, I., Tachos, N. S., et al.  
1512 (2021). Review of eye tracking metrics involved in emotional and cognitive processes. *IEEE Reviews in  
1513 Biomedical Engineering* 16, 260–277
- 1514 Smit, A. and Van Gisbergen, J. (1990). An analysis of curvature in fast and slow human saccades.  
1515 *Experimental Brain Research* 81, 335–345
- 1516 Smit, A., Van Gisbergen, J., and Cools, A. (1987). A parametric analysis of human saccades in different  
1517 experimental paradigms. *Vision research* 27, 1745–1762
- 1518 Snyder, L. H., Calton, J. L., Dickinson, A. R., and Lawrence, B. M. (2002). Eye-hand coordination:  
1519 saccades are faster when accompanied by a coordinated arm movement. *Journal of neurophysiology* 87,  
1520 2279–2286
- 1521 Souto, D. and Kerzel, D. (2014). Ocular tracking responses to background motion gated by feature-based  
1522 attention. *Journal of neurophysiology* 112, 1074–1081
- 1523 Sparks, D. L. (1986). Translation of sensory signals into commands for control of saccadic eye movements:  
1524 role of primate superior colliculus. *Physiological reviews* 66, 118–171
- 1525 Spering, M. (2022). Eye movements as a window into decision-making. *Annual review of vision science*  
1526 8, 427–448
- 1527 Spering, M. and Gegenfurtner, K. R. (2007). Contextual effects on smooth-pursuit eye movements. *Journal  
1528 of Neurophysiology* 97, 1353–1367
- 1529 Startsev, M. and Zemblys, R. (2023). Evaluating eye movement event detection: A review of the state of  
1530 the art. *Behavior Research Methods* 55, 1653–1714
- 1531 Steinman, R. M. (1965). Effect of target size, luminance, and color on monocular fixation. *JOSA* 55,  
1532 1158–1164
- 1533

- 1534 Steinman, R. M., Kowler, E., and Collewijn, H. (1990). New directions for oculomotor research. *Vision*  
1535 *research* 30, 1845–1864
- 1536 Stoica, P., Moses, R. L., et al. (2005). *Spectral analysis of signals*, vol. 452 (Pearson Prentice Hall Upper  
1537 Saddle River, NJ)
- 1538 Stolte, M., Kraus, L., and Ansorge, U. (2023). Visual attentional guidance during smooth pursuit eye  
1539 movements: Distractor interference is independent of distractor-target similarity. *Psychophysiology*,  
1540 e14384
- 1541 Stubbs, J. L., Corrow, S. L., Kiang, B., Panenka, W. J., and Barton, J. J. (2018). The effects of enhanced  
1542 attention and working memory on smooth pursuit eye movement. *Experimental brain research* 236,  
1543 485–495
- 1544 Troost, B. T. and Daroff, R. B. (1977). The ocular motor defects in progressive supranuclear palsy. *Annals*  
1545 *of Neurology: Official Journal of the American Neurological Association and the Child Neurology*  
1546 *Society* 2, 397–403
- 1547 Tychsen, L. and Lisberger, S. G. (1986). Visual motion processing for the initiation of smooth-pursuit eye  
1548 movements in humans. *Journal of neurophysiology* 56, 953–968
- 1549 Underwood, G., Binns, A., and Walker, S. (2000). Attentional demands on the processing of neighbouring  
1550 words. In *Reading as a perceptual process* (Elsevier). 247–268
- 1551 Van Donkelaar, P. and Drew, A. S. (2002). The allocation of attention during smooth pursuit eye movements.  
1552 *Progress in brain research* 140, 267–277
- 1553 Van Gelder, P., Lebedev, S., Liu, P. M., and Tsui, W. H. (1995). Anticipatory saccades in smooth pursuit:  
1554 task effects and pursuit vector after saccades. *Vision Research* 35, 667–678
- 1555 Van Gisbergen, J., Van Opstal, A., and Roebroek, J. (1987). Stimulus-induced midflight modification of  
1556 saccade trajectories. In *Eye movements From physiology to cognition* (Elsevier). 27–36
- 1557 Van Opstal, A. and Van Gisbergen, J. (1987). Skewness of saccadic velocity profiles: a unifying parameter  
1558 for normal and slow saccades. *Vision research* 27, 731–745
- 1559 van Opstal, A. J. and Goossens, H. (2008). Linear ensemble-coding in midbrain superior colliculus  
1560 specifies the saccade kinematics. *Biological cybernetics* 98, 561–577
- 1561 Van Orden, K. F., Jung, T. P., and Makeig, S. (2000). Combined eye activity measures accurately estimate  
1562 changes in sustained visual task performance. *Biol. Psychol.*, 221–240
- 1563 Viviani, P. (1977). Berthoz a, and tracey d. *The curvature of oblique saccades*. *Vision Res* 17, 661–664
- 1564 Viviani, P. and Swensson, R. G. (1982). Saccadic eye movements to peripherally discriminated visual  
1565 targets. *Journal of Experimental Psychology: Human Perception and Performance* 8, 113
- 1566 von Wartburg, R., Wurtz, P., Pflugshaupt, T., Nyffeler, T., Lüthi, M., and Müri, R. M. (2007). Size matters:  
1567 Saccades during scene perception. *Perception* 36, 355–365
- 1568 Vullings, C. (2018). *Saccadic latencies depend on functional relations with the environment*. Ph.D. thesis,  
1569 Université de Lille
- 1570 Walker, R., McSorley, E., and Haggard, P. (2006). The control of saccade trajectories: Direction of curvature  
1571 depends on prior knowledge of target location and saccade latency. *Perception & Psychophysics* 68,  
1572 129–138
- 1573 Wang, Y. and Cong, W. (2015). Statistical analysis of air traffic controllers' eye movements. In *Conference:*  
1574 *Air Traffic Management R&D Seminar*
- 1575 Welch, P. (1967). The use of fast fourier transform for the estimation of power spectra: A method based on  
1576 time averaging over short, modified periodograms. *IEEE Transactions on Audio and Electroacoustics*  
1577 15, 70–73

- 1578 Wetzel, P. A., Gitchel, G. T., and Baron, M. S. (2011). Effect of parkinson's disease on eye movements  
1579 during reading. *Investigative Ophthalmology & Visual Science* 52, 4697–4697
- 1580 Whelan, R. (2008). Effective analysis of reaction time data. *The psychological record* 58, 475–482
- 1581 Xu-McGregor, D. K. and Stern, J. A. (1996). Time on task and blink effects on saccade duration.  
1582 *Ergonomics* 39, 649–660
- 1583 Xu-Wilson, M., Zee, D. S., and Shadmehr, R. (2009). The intrinsic value of visual information affects  
1584 saccade velocities. *Exp. Brain Res.* 196, 475–481
- 1585 Yarbus, A. L. and Yarbus, A. L. (1967). Eye movements during perception of complex objects. *Eye*  
1586 *movements and vision*, 171–211
- 1587 Yee, R. D., Cogan, D. G., Zee, D. S., Baloh, R. W., and Honrubia, V. (1976). Rapid eye movements in  
1588 myasthenia gravis: II. electro-oculographic analysis. *Archives of ophthalmology* 94, 1465–1472
- 1589 Zackon, D. H. and Sharpe, J. A. (1987). Smooth pursuit in senescence: effects of target acceleration and  
1590 velocity. *Acta oto-laryngologica* 104, 290–297
- 1591 Zemblys, R., Niehorster, D. C., Komogortsev, O., and Holmqvist, K. (2018). Using machine learning to  
1592 detect events in eye-tracking data. *Behavior research methods* 50, 160–181
- 1593 Zuber, B., Semmlow, J., and Stark, L. (1968). Frequency characteristics of the saccadic eye movement.  
1594 *Biophysical Journal* 8, 1288–1298